


RESEARCH ARTICLE

WILEY



Mesencephalic dopamine neurons interfacing the shell of nucleus accumbens and the dorsolateral striatum in the rat

Floris G. Wouterlood¹  | Angela Engel¹ | Mariah Daal¹ | Gertjan Houwen¹ |
 Aileen Meinders¹ | Tomàs Jordà Siquier¹ | Jeroen A. M. Beliën² |
 Yvette C. van Dongen^{1,3} | Jørgen Scheel-Krüger⁴ | Anne-Marie Thierry³ |
 Henk J. Groenewegen¹ | Jean-Michel Deniau³

¹Department of Anatomy & Neurosciences, VU University Medical Center, Neuroscience Campus Amsterdam, 1007 MB Amsterdam, The Netherlands

²Department of Pathology, VU University Medical Center, Neuroscience Campus Amsterdam, 1007 MB, Amsterdam, The Netherlands

³Institut National de la Santé et de la Recherche Médicale, U114, Chaire de Neuropharmacologie, Collège de France, 11 Place Marcelin Berthelot, 75231 Paris Cedex 05, France

⁴Department of Clinical Medicine, Center of Functionally Integrative Neuroscience, Nørrebrogade 44, 8000 Aarhus C, Denmark

Correspondence

Floris G. Wouterlood, Department of Anatomy & Neurosciences, Vrije Universiteit Medical Center, P.O. Box 7057, 1007 MB Amsterdam, The Netherlands.
 Email: FG.Wouterlood@vumc.nl; floris256@yahoo.com

Abstract

Parallel corticostriatonigral circuits have been proposed that separately process motor, cognitive, and emotional-motivational information. Functional integration requires that interactions exist between neurons participating in these circuits. This makes it imperative to study the complex anatomical substrate underlying corticostriatonigral circuits. It has previously been proposed that dopaminergic neurons in the ventral mesencephalon may play a role in this circuit interaction. Therefore, we studied in rats convergence of basal ganglia circuits by depositing an anterograde neuroanatomical tracer into the ventral striatum together with a retrograde fluorescent tracer ipsilaterally in the dorsolateral striatum. In the mesencephalon, using confocal microscopy, we looked for possible appositions of anterogradely labeled fibers and retrogradely labeled neurons, “enhancing” the latter via intracellular injection of Lucifer Yellow. Tyrosine hydroxylase (TH) immunofluorescence served to identify dopaminergic neurons. In neurophysiological experiments, we combined orthodromic stimulation in the medial ventral striatum with recording from ventral mesencephalic neurons characterized by antidromic stimulation from the dorsal striatum. We observed terminal fields of anterogradely labeled fibers that overlap populations of retrogradely labeled nigrostriatal cell bodies in the substantia nigra pars compacta and lateral ventral tegmental area (VTA), with numerous close appositions between boutons of anterogradely labeled fibers and nigrostriatal, TH-immunopositive neurons. Neurophysiological stimulation in the medial ventral striatum caused inhibition of dopaminergic nigrostriatal neurons projecting to the ventrolateral striatal territory. Responding nigrostriatal neurons were located in the medial substantia nigra and adjacent VTA. Our results strongly suggest a functional link between ventromedial, emotional-motivational striatum, and the sensorimotor dorsal striatum via dopaminergic nigrostriatal neurons.

KEYWORDS

dopaminergic neurons, inhibition, neuroanatomical tracing, neurophysiology, striato-mesostriatal loops

This is an open access article under the terms of the Creative Commons Attribution-NonCommercial License, which permits use, distribution and reproduction in any medium, provided the original work is properly cited and is not used for commercial purposes.

© 2018 The Authors Journal of Neuroscience Research Published by Wiley Periodicals, Inc.

Significance

We demonstrate here with anatomical and neurophysiological methods in rats that neurons in the ventral striatum exhibit inhibitory influence on neurons located in the dorsolateral striatum. This inhibitory circuit is monosynaptic via dopaminergic neurons in the substantia nigra of the mesencephalon. The anatomical substrate of this inhibition is formed by boutons of fibers originating in the ventral striatum that appose dendrites of mesencephalic dopaminergic neurons, sometimes in a very conspicuous configuration: the “earmuff” type of contact (EMC). Functionally, this implies a link between the emotional-motivational and sensorimotor domains of the striatum, mediated by mesencephalic dopaminergic neurons residing in substantia nigra and ventral tegmental area.

1 | INTRODUCTION

The basal ganglia (striatum, pallidum, subthalamic nucleus, and substantia nigra), contain neuronal circuits that interconnect cerebral cortical and subcortical structures in the fore-brain and midbrain (Gerfen, 2004; Gerfen & Bolam, 2017). Main circuits lead from all parts of the cerebral cortex via basal ganglia-thalamocortical loops back to premotor and prefrontal cortical areas. The striatum is considered to form the major input structure of the basal ganglia (Gerfen & Bolam, 2017; Groenewegen, Voorn, & Scheel-Krüger, 2016). Outputs from the basal ganglia to the thalamus and brainstem originate from the internal part of the globus pallidus and the substantia nigra pars reticulata (SNr). Intrinsic basal ganglia connections consist of reciprocal projections between virtually all basal ganglia nuclei with a predominance for striatal projections to output structures mentioned above (the “direct” striatal pathway) and a second pathway from the striatum via the external globus pallidus and subthalamic nucleus to the output structures (the “indirect” pathway). Apart from cortical afferents, the striatum receives projections from midline and intralaminar thalamic nuclei, amygdala, and monoaminergic cell groups in the brainstem. The thalamic and monoaminergic inputs in the striatum modulate information transfer in the basal ganglia-thalamocortical loops.

If we focus on the functional signature of the various cortical afferents of the striatum, then the dorsal portion of the striatum, globally coinciding with the caudate nucleus and putamen, seems to be mainly involved in sensorimotor and cognitive processing while its ventral portion processes information associated with appetitively and aversively motivating information in the context of action selection (reviewed by Floresco, 2015; Sesack & Grace, 2010; Voorn, Vanderschuren, Groenewegen, Robbins, & Pennartz, 2004). Information from functionally distinct cortical areas can be processed in separate territories of the striatum via their respective associated striatonigral and striatopallidal pathways (parallel cortico-basal ganglia circuits; Alexander & Crutcher, 1990; Deniau & Thierry, 1997; Groenewegen, Wright, Beijer, & Voorn, 1999; Maily et al., 2001). Interrelationships between functionally different circuits as well as integration of information must occur somewhere in the organization of parallel circuits in order to produce meaningful and

integrated motor, cognitive and behavioral output of the forebrain. At which level this integration occurs is an important issue. Varying, but notably specific degrees of overlap between functionally different cortical projections at the level of the striatum may play an important role (Calzavara, Maily, & Haber, 2007; Groenewegen et al., 2016; Maily, Aliane, Groenewegen, Haber, & Deniau, 2013). However, also the projections from the dopaminergic (DA) cell groups in the ventral mesencephalon, that is, the ventral tegmental area (VTA; containing the dopaminergic cell group A10) and substantia nigra pars compacta (SNc; containing the dopaminergic cell group A9), to different parts of the striatum must be considered (Haber, Fudge, & McFarland, 2000; Menegas et al., 2015).

Histochemical and anatomical studies have established that the major component of the ventral striatum, that is, the nucleus accumbens (Acb), consists of two main subdivisions, the core (Acb-c) and shell (Acb-s), each with distinctive connective characteristics (reviews: Groenewegen et al., 2016; Heimer et al., 1997). Acb-c resembles the dorsal striatum in that it receives major fiber input from the cerebral cortex, that is, medial and lateral prefrontal areas, while it projects to the sub-commissural ventral pallidum and the SNr. Acb-s, by contrast, receives major inputs from the hippocampus and the amygdaloid complex while it innervates (besides the ventral pallidum) predominantly VTA and SNc (Deniau, Menetrey, & Charpier, 1996; Geisler & Zahm, 2005; Groenewegen et al., 1999; Heimer, Zahm, Churchill, Kalivas, & Wohltmann, 1991; Heimer et al., 1997; Maurice, Deniau, Menetrey, Glowinski, & Thierry, 1997, 1998; Montaron, Deniau, Menetrey, Glowinski, & Thierry, 1996; Tripathi, Prensa, Cebrián, & Mengual, 2010; Usuda, Tanaka, & Chiba, 1998; Volman et al., 2013; Wright, Beijer, & Groenewegen, 1996; Xia et al., 2011; Zahm et al., 2011). A comparative three-dimensional (3D) analysis in the rat of the striatonigral and nigrostriatal projections revealed that each functional territory of the dorsal striatum is innervated by a separate subpopulation of VTA/SNc neurons (Maurin, Banrezes, Menetrey, Maily, & Deniau, 1999). A “proximal” neuron subpopulation located in SNc occupies for instance a position in register with the striatonigral projections in the subjacent SNr. A close spatial relationship like this suggests that “proximal” neurons are involved in reciprocal striato-nigrostriatal feedback circuits while neurons belonging to a “distal” subpopulation located medially and dorsally in SNc and VTA are likely involved in nonreciprocal connections with the dorsal striatum.

Dopaminergic neurons in SNc and VTA densely innervate the striatum. Based on the observation that Acb innervates VTA and SNc, Nauta, Smith, Faull, and Domesick (1978) proposed that dopaminergic neurons in VTA and SNc constitute an interface between limbic and extrapyramidal motor systems. In line with this, Mogenson, Jones, and Yim (1980) proposed that the Acb plays an important role in the motivational influence on actions (“from motivation to action”). However, Nauta’s conclusions were based on rather indirect, light microscopic observations, like those of later studies in primates (Haber et al., 2000). Thus, the position of mesencephalic dopaminergic neurons in basal ganglia-thalamocortical neuronal circuits needed further clarification. In this respect, Somogyi, Bolam, Totterdell, and Smith (1981), in a lesion-electron microscopy (lesion-EM) study, were the first to demonstrate synaptic contacts between terminals of ventral striatal efferents and dendrites of nigral neurons projecting to the dorsal striatum. Xia et al.

(2011), with an optogenetic approach, found evidence in ex vivo slice preparations suggesting that non-dopaminergic VTA neurons are involved in this circuitry. At the same time, Chuhma, Tanaka, Hen, and Rayport (2011) reported in transgenic mice strong responses from substantia nigra GABA neurons simultaneously with poor responses from SNc dopaminergic neurons after photostimulation of incoming striatal fibers, indicating a low functional connectivity of SNc dopaminergic neurons. Previously, cocaine stimulation of the mesoaccumbens system had led to a similar conclusion (Einhorn, Johansen, & White, 1998).

In the present study, we investigated to which extent neurons in Acb exert direct synaptic influence on the “proximal” and “distal” subpopulations of nigrostriatal neurons projecting to the sensorimotor dorsal striatum. This question has become relevant since in addition to the observations by Einhorn et al. (1998) and Chuhma et al. (2011), Menegas et al. (2015) raise the question whether striato-nigro-striatal loops involving dopaminergic SN neurons should be considered “open” or “closed.” For the purpose of studying the role of mesencephalic dopaminergic neurons in striato-nigro-striatal circuits, we conducted several series of experiments. Anterograde neuroanatomical tracer injected in various locations in the striatum was combined with fluorescence neurochemical phenotyping (Wouterlood, Bloem, Mansvelter, Luchicchi, & Deisseroth, 2014) to visualize striatomesencephalic projections simultaneously with potential target neurons in SN. In other experiments, we combined small injections of anterograde tracer into Acb-c and Acb-s with retrograde tracing from the dorsolateral striatal territory innervated by the sensorimotor cortical areas. As VTA and SN neurons possess long dendrites that extend far into territories adjacent to VTA and SN, it was essential here to render dendritic trees of dopaminergic neurons completely visible. To this aim, we conducted in this group of experiments postmortem intracellular injection of Lucifer Yellow (LY) into retrogradely labeled neurons. Thus, we could obtain essential anatomical information where it comes to the questions left by the studies by Einhorn et al. (1998) and Chuhma et al. (2011). In parallel, we conducted a series of neurophysiological experiments to study the effects of electrical stimulation of the Acb shell on dopaminergic nigrostriatal neurons projecting to the orofacial, ventrolateral striatum. Preliminary neuroanatomical tracing and neurophysiological results have been published previously (Thierry et al., 2002; van Dongen, Kolomiets, Groenewegen, Thierry, & Deniau, 2009).

2 | MATERIALS AND METHODS

All experimental procedures were performed in accordance with European Community Council Directive 86/609/EEC and in obedience of all additional national and local rules governing animal research. The minimum number of experimental animals was used. In total, we used 41 rats. Neuroanatomical tracing experiments were performed in the Amsterdam lab with Wistar rats ($n = 23$, including one legacy injection case [experiment 90468] used for electron microscopy). Neurophysiological recordings were obtained in the Paris lab ($n = 18$; Sprague-Dawley rats). Experimental animals were housed in the respective institutional animal facilities. Their health and well-being were inspected twice a day. In the Amsterdam

animal facility, the animals were during one of these inspections gently taken out of their cages and handled during approximately 5 min.

2.1 | Anatomical tracing studies

2.1.1 | Groups, surgical procedure, tracers, and tracer delivery

All rats used in the anatomical tracing studies were females, body weight 180–240 g; Harlan/CPB, Zeist, Netherlands. Experiments were divided into three groups: Group A: anterograde tracer injected in a dorsal striatum locus, Group B: anterograde tracer injected in a ventral striatum locus, and Group C: anterograde tracer injected in a ventral striatum locus together with retrograde tracer deposition in the ipsilateral dorsal striatum. In order to reduce the number of experimental animals, we injected in several subjects (2012-001, 2012-002, 2012-004, and 2012-005) *Phaseolus vulgaris-Leucoagglutinin* (PHA-L) in one cerebral hemisphere and biotinylated dextran amine (BDA) contralaterally. In rat 1009, we injected BDA bilaterally. Injection spots, with an indication which tracer was used, are presented in Figures 1–3 and 5. Injection spot coordinates of all experiments are provided in Table 1.

Initially, animals were anesthetized prior to surgery with an intraperitoneal injection of a 4:3 mixture of a 1% solution of ketamine (Aesco, Boxtel, Netherlands) and a 2% solution of xylazine (Bayer, Brussels, Belgium), injected intramuscularly (1 ml/kg). In 2010, inhalation anesthesia procedures were introduced at the Amsterdam animal housing facility to improve animal well-being. Complying with these procedures, we continued with the new anesthesia (rat numbers 2010-nn and 2012-nn): initially a mixture of 3% isoflurane-O₂ (0.3 L/min) and N₂O (0.6 L/min) was given; after stabilization, we maintained a flow of 1.25–2.5% isoflurane-O₂ (0.75 L/min) and N₂O (1.5 L/min). Body temperature (36–37°C) was maintained with a homeothermic mat. Anaesthetized animals were mounted in a stereotaxic frame. Local anesthesia (10% lidocaine) was applied to the skin at the site of incision and a trephine opening made in the skull.

Anterograde tracers used were BDA (10,000 MW, Invitrogen-Molecular Probes, Eugene, OR; 5% in 100 mM phosphate buffer (PB), pH 7.4 and PHA-L (Vector Labs, Burlingame, VT; 2.5% PHA-L in 50 mM Tris-buffered saline, pH 7.4). Tracer was delivered through a glass micropipette (external tip diameter 20 μ m), using a positive pulsed DC current of 6 μ A (7 s on/off) (Midgard CCS-3 constant current source, USA) (delivery of the tracer 2–5 min; micropipette remaining 5 min in situ to avoid track labeling). Stereotaxic coordinates were derived from the rat brain atlas by Paxinos and Watson (2005).

For retrograde tracing, we used 2% FluoroGold (FG, Fluorochrome Inc., Denver, CO; www.fluorochrome.com) in 100 mM cacodylate buffer, pH 7.3. A volume of 0.1–0.2 μ l of FG was mechanically delivered through a Hamilton syringe. After surgery, the animals were allowed to recover and then returned to their home cage.

2.2 | Histological procedures

2.2.1 | Fixation, sectioning, and storage

Seven days after the surgery the subjects were deeply anesthetized via intraperitoneal injection with sodium pentobarbital (Nembutal,

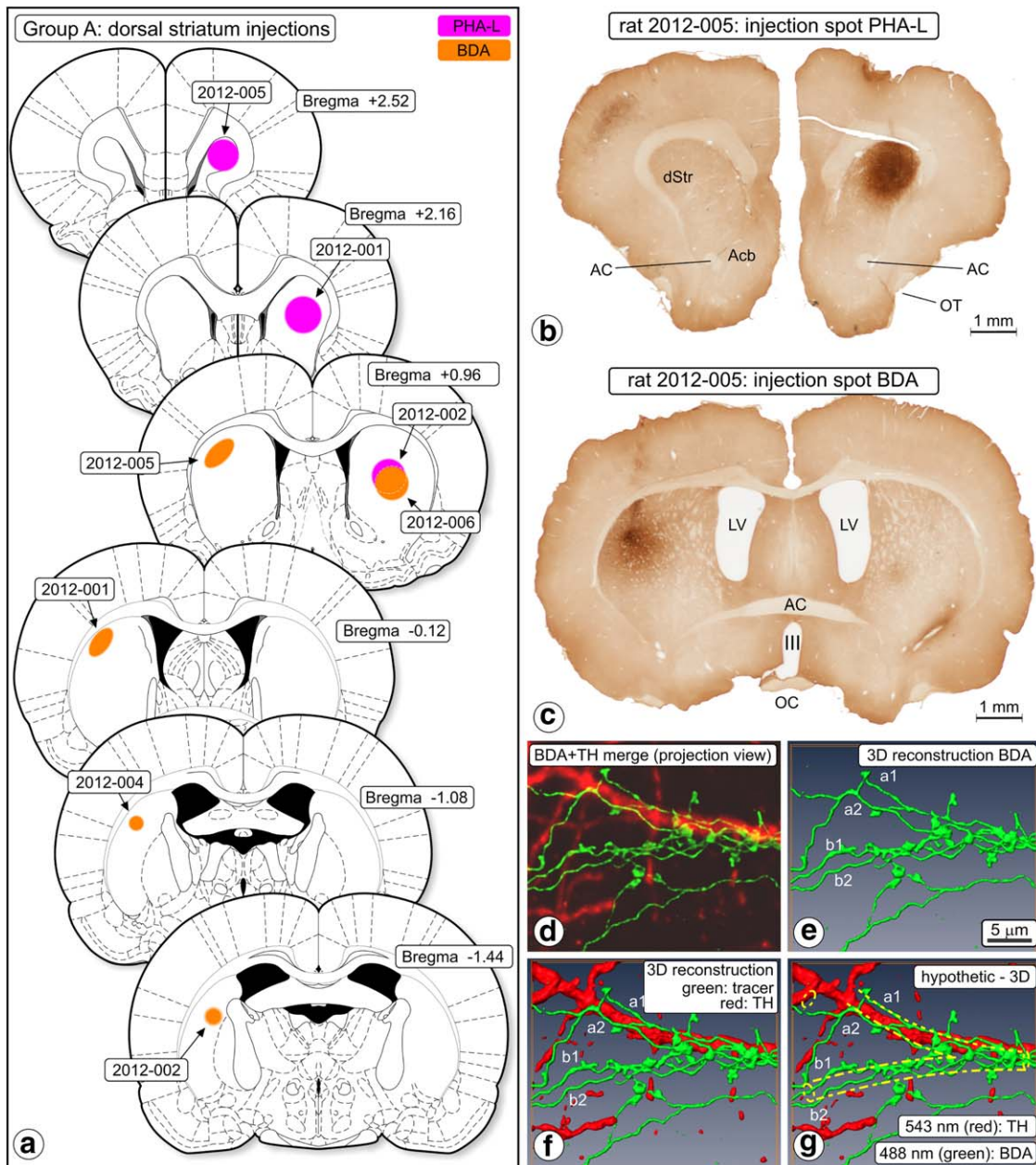


FIGURE 1 Anterograde tracing, dorsal striatum injections (Group A). (a) Chartings of injection sites. (b) Photomicrograph of a section of experiment 2012-005 showing the center of the *Phaseolus vulgaris-Leucoagglutinin* (PHA-L) injection spot. (c) In the same animal and more caudally, biotinylated dextran amine (BDA) was injected into the contralateral hemisphere. III = third ventricle; AC = anterior commissure; Acb = nucleus accumbens; LV = lateral ventricle; OT = olfactory tract. (d–g) “Woolly” fibers. BDA-labeled fibers and their boutons in ventral tegmental area (VTA), rat 2010-006. The “woolly” configuration here consists of two fibers (a,b) running parallel on each side of an (unstained, i.e., imaginary) dendrite, wrapping around that dendrite and forming boutons. (d) Merged projection view of the images obtained in two-channel confocal scanning (BDA green, TH red). (e) 3D reconstruction of the BDA labeled fibers, (f) merged 3D reconstruction; BDA-labeled fibers and TH expressing structures. (g) Hypothesized dendrite added (yellow dashed lines). Scale marker in (e) holds for all frames. “Woolly” fiber terminals were in all our observations involved with an “invisible dendrite” and never with a TH-immunopositive dendrite [Color figure can be viewed at wileyonlinelibrary.com]

60 mg/kg body weight, i.p.; Ceva, Paris, France) and transcardially perfused briefly with 0.9% saline followed by 250 ml of 4% freshly depolymerized paraformaldehyde (Merck, Darmstadt, Germany) and 0.05% glutaraldehyde (Merck-Schuchardt, Hohenbrunn, Germany) in PB (100–125 mM, pH 7.0, room temperature). After removal, each brain was post-fixed for 1.5 hr, cryoprotected with 20% glycerin (Merck) mixed with 2% dimethyl sulfoxide (DMSO;

Merck) in PB (0.1 M, pH 7.4) (18–48 hr at 4°C) and sectioned horizontally or transversely on a sliding freezing microtome at a thickness of 40 μm. Sections were collected in vials containing either PB (0.1 M, pH 7.4) for direct processing, or in vials with the glycerin DMSO-PB medium for storage at –20°C. Brains used for intracellular LY injection (Group C rats) were always sectioned in the transverse plane into slices with alternating thickness (100 and 500 μm),

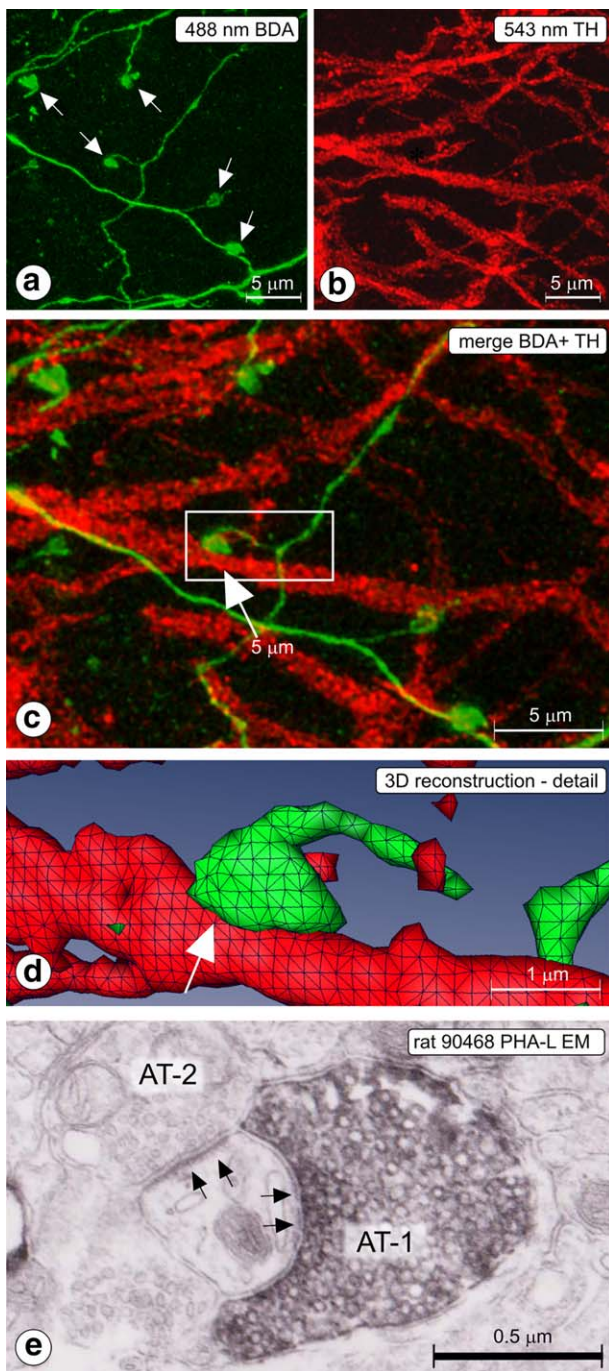


FIGURE 2 (a–d) Rat 2012-006; CLSM sample acquired in substantia nigra pars reticulata (SNr). (a) 488 nm channel; Z projected image showing labeled, thin fibers, and boutons (arrows), (b) 543 nm channel; Z projected image showing tyrosine hydroxylase (TH) immunofluorescent dendrites. (c) Z-projected merge image. BDA = green, TH = red. Apposition between labeled fiber and TH dendrite is indicated with an arrow. The boxed area is enlarged and presented in 3D reconstruction in (d). Apposition indicated in frames (c) and (d) with arrow. Such appositions are suggestive for the existence of a synapse. (e) Rat 90468; electron micrograph taken in SNr (injection of PHA-L in Acb-c, see Figure 5a), showing a synapse (arrows) between the *Phaseolus vulgaris*-*Leucoagglutinin*-labeled axon terminal (AT-1) and a thin dendrite. The same dendrite receives also a synaptic contact from an axon terminal of unknown origin (AT-2) [Color figure can be viewed at wileyonlinelibrary.com]

with a vibrating microtome (Leica VT1000S, Jena, Germany). These slices were collected in PB and parked in a refrigerator.

2.2.2 | Immunofluorescence staining and complementary neurochemical phenotyping

Brain sections of rats in which PHA-L had been injected were incubated with a cocktail of goat anti-PHA-L antibody (Vector, 1:1,000) mixed with mouse anti-tyrosine hydroxylase antibody (TH; MAB 318; Chemicon, Temecula, CA, 1:1,000) for 48 hr at room temperature, rinsed, and then incubated with a cocktail of IgG's developed in donkey: anti-goat-Alexa Fluor 488, anti-mouse-Alexa Fluor 546. Brain sections of rats in which BDA had been injected were incubated with the mouse MAB318 antibody against TH (1:1,000) for 48 hr at room temperature, rinsed and then incubated with a cocktail of 1:400 streptavidin-Alexa Fluor 546 (Invitrogen-Molecular Probes; Alexa Fluor is a trade mark of this company) and 1:400 goat anti-mouse-Alexa Fluor 633 (Invitrogen-Molecular Probes).

In several BDA tracing experiments, we added an extra antibody to the primary antibody cocktail: rabbit anti-vesicular GABA transporter (VGAT; cat nr. 131002; Synaptic Systems, Göttingen, Germany; 1:500). Binding of the latter antibody was detected with anti-rabbit-Alexa Fluor 633 developed in goat (1:400; Invitrogen-Molecular Probes). In these experiments, the binding of the mouse anti-TH primary antibody was tested with donkey-anti mouse Alexa Fluor 488. This triple staining was done to determine whether labeled efferent striatal fibers were GABAergic. Accumulation of VGAT immunosignal in axonal swellings ("boutons," see below) is indicative for the involvement of this bouton in a synaptic contact. VGAT is considered as a marker for GABA-mediated synaptic transmission (Chaudhry et al., 1998).

2.2.3 | Mapping BDA injection sites: Calbindin-D28kDA or MOR immunohistochemistry

Recognizing BDA injection sites in relation to immunohistochemical landmarks indicating subregions of Acb (shell or core) was achieved via double staining for BDA and either calbindin-D28k (CaB) or μ -opioid receptor (MOR). The immunohistochemical staining followed exactly the above procedure except that in lieu of the anti-TH antibody we used a monoclonal mouse anti-CaB antibody (Sigma, St. Louis, MO), or a goat anti-MOR1 (C-20; Santa Cruz, cat nr. SC-7488). For the detection of bound CaB, we used goat anti-mouse IgG (Sigma) and goat peroxidase-anti peroxidase (Sigma) (procedure described in full by Wright et al., 1996). Bound anti-MOR was detected with donkey-anti goat IgG-Alexa Fluor 546.

2.2.4 | Intracellular injection in slices of fixed brain

The 100- μ m thick slices of Group C rat brains were used for documentation purposes: the distribution of BDA labeled fibers in the mesencephalon, the relationships of these fibers with retrogradely FG labeled neurons in the VTA and SN, and the topography of BDA labeled fibers with respect to the A9 and A10 cell groups as identified via additional TH immunofluorescence staining. To accomplish this, slices were rinsed with TBS-TX and incubated overnight at room temperature with mouse monoclonal anti-TH antibody (1:1,000, ImmunoStar, Hudson, WI) and, after rinsing with TBS-TX, for 1 hr with a mixture of goat-anti mouse

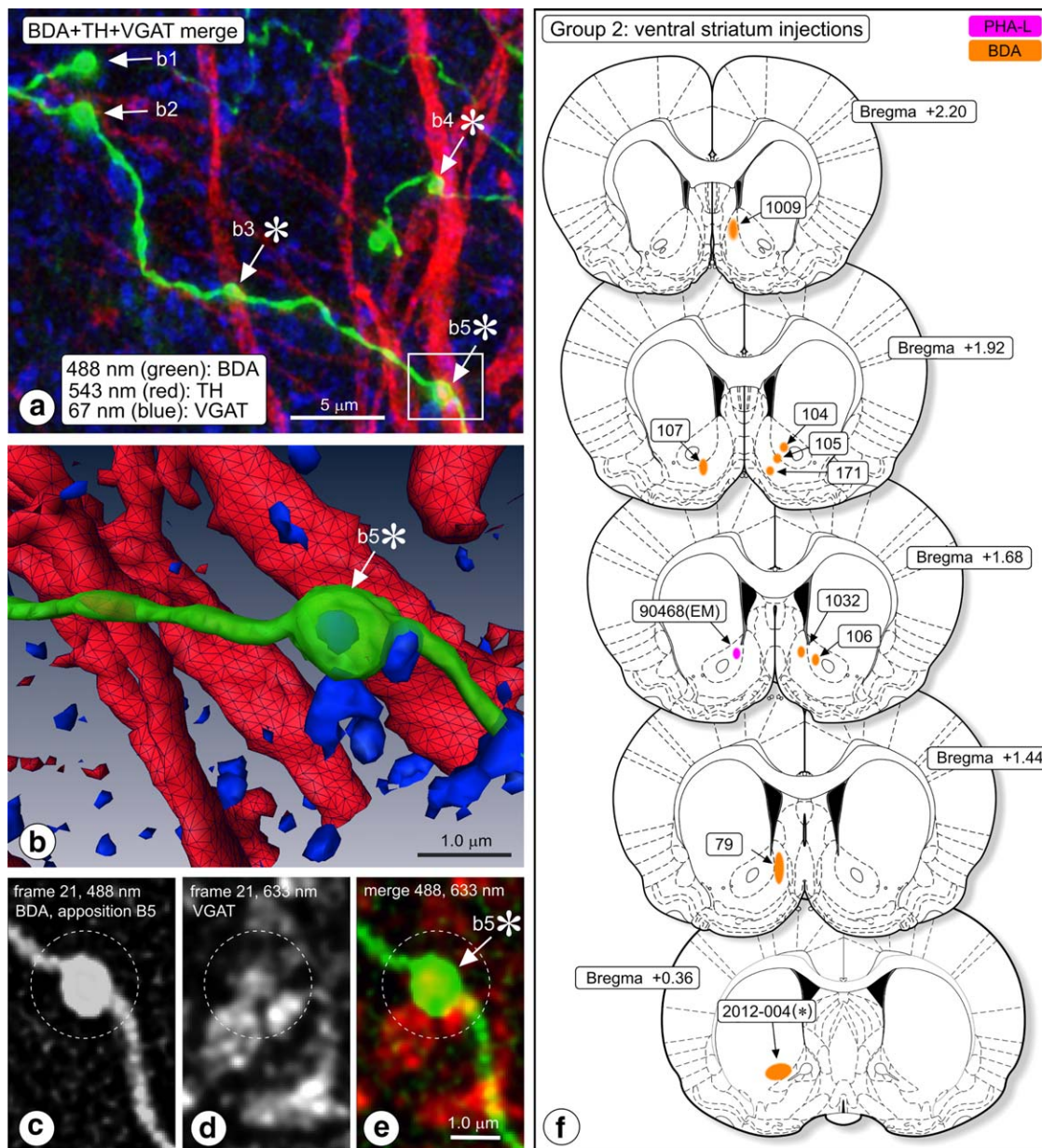


FIGURE 3 (a–e) Triple-immunofluorescence image acquisition in substantia nigra pars reticulata (SNr) of rat #107. (a) Merge image, showing appositions of boutons of biotinylated dextran amine (BDA) labeled fibers (green; arrows) with TH-expressing dendrites (red). VGAT immunosignal is blue. Merge image produced by deconvoluting image stacks, Z-projecting and then merging. Boutons b3, b4, and b5 appose a TH expressing dendrite (asterisks). (b) 3D reconstruction of this image series, zooming in on bouton b5. The interior of this bouton is enriched with VGAT immunofluorescence signal (blue; colocalization). (c–e) Frames nr 21 in the 488 nm, and 633 nm channels (stack of 60 frames in three channels) were extracted from the image series and are shown here. (c) Frame 21 in the 488 nm channel (BDA), (d) frame 21 in the 633 nm channel (VGAT). (e) Color coded merge image documenting that the BDA labeled bouton nr b5 (here color code green) “colocalizes” with VGAT signal (here color coded red). (f) Anterograde tracing, ventral striatum injections (Group B). Chartings of injection sites. Injections, except cases 104, 106, and the “EM” injection (90468), centered in the shell of Acb (Acb-s) [Color figure can be viewed at wileyonlinelibrary.com]

IgG-Alexa Fluor 633 (Invitrogen-Molecular Probes) and streptavidin-Alexa Fluor 546 (Invitrogen-Molecular Probes). They were then mounted on glass slides, dried, and coverslipped.

The 500- μ m thick slices were rinsed in PB and transferred to a small Petri dish mounted in the intracellular injection unit: a Zeiss fluorescence microscope equipped with long-working distance objectives, a micromanipulator, and an iontophoretic injection device capable of delivering current in the nA range (detailed description by Buhl,

Schwerdtfeger, Germroth, & Singer, 1989; Shi & Cassell, 1993; Wouterlood, Goede, Arts, & Groenewegen, 1992; equipment refined by Kajiwara et al., 2008). Intracellular filling of retrogradely FG labeled cells in the mesencephalon (VTA, SN) was achieved via impalement of their cell bodies with a glass pipette (microelectrode; tip diameter in the 0.5–0.8 μ m range; resistance 70–130 M Ω) containing 4% LY dilithium salt (Invitrogen-Molecular Probes). After approaching and impaling prospective cells, a negative current was applied to the micropipette (2 nA,

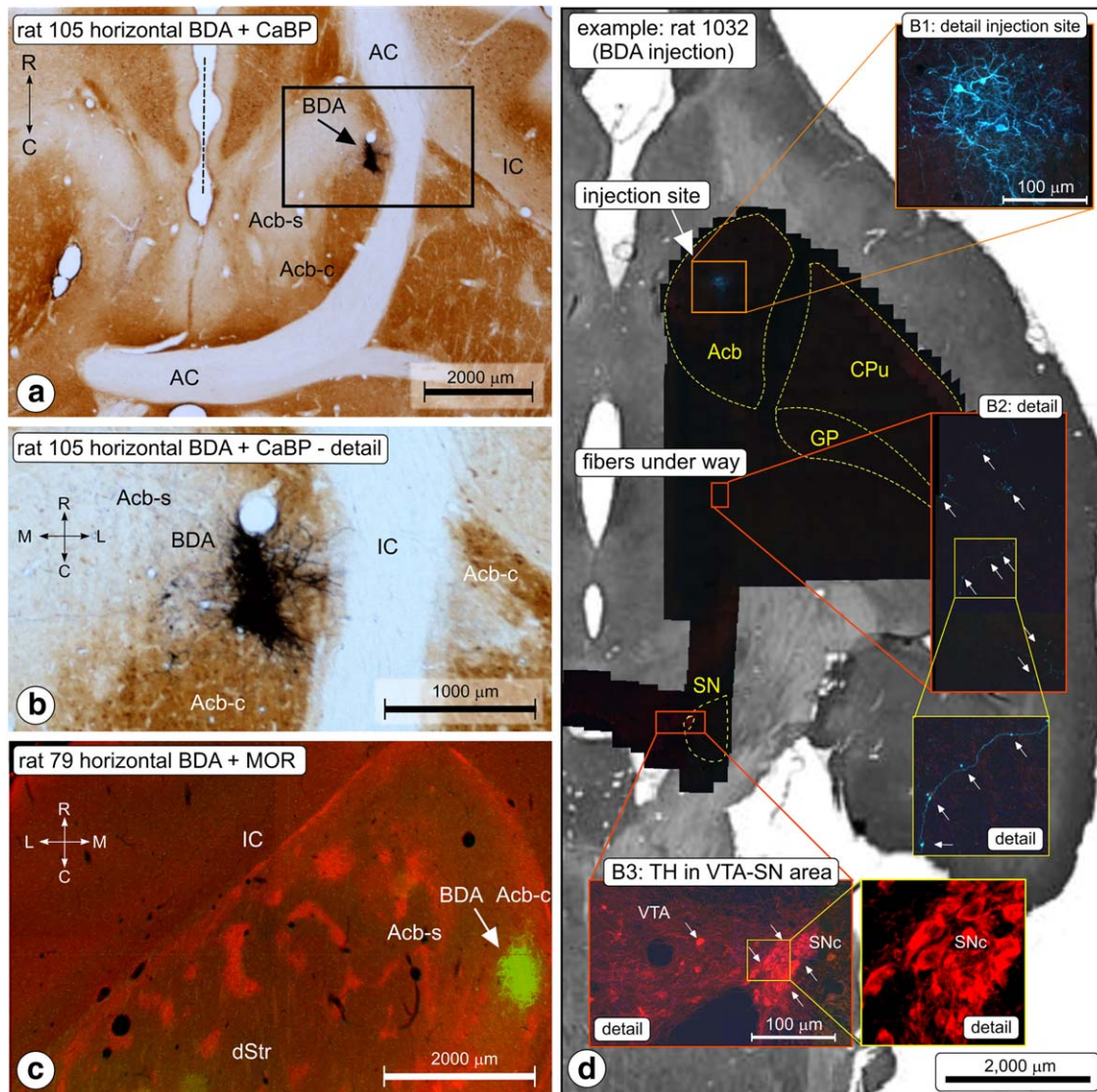


FIGURE 4 Anterograde tracing in Group B (ventral striatum injections; nucleus accumbens, Acb). (a) Photomicrograph of the (biotinylated dextran amine [BDA]) injection site in rat nr 105. Horizontal section of the forebrain, BDA (blue-black)–CaB (brown) double staining. Acb-c is characterized by dense CaB staining. The center of the BDA injection spot (arrow) is located medial to the anterior limb of the anterior commissure (AC). The midline is indicated with the dashed line. IC = internal capsule. (b) Higher magnification of the injection site shown in (a). (c) BDA injection site in a horizontal section in rat nr 79. Double immunofluorescence imaging (green: BDA green, red: μ -opioid receptor distribution). (d) Tracking the procedure: montage of injection site- and fiber-pathway mapping in case 1032, sample image acquisition and postacquisition counterstaining. Sections include both the injection site of the tracer in Acb-s, the descending route taken by the fibers and the substantia nigra (SN). After the double immunofluorescence procedure, scanning, and sampling this section was Nissl counterstained and photographed (background image). Final illustration produced by overlaying all low-res and high-res images [Color figure can be viewed at wileyonlinelibrary.com]

500 ms on, 50 ms off), for at least 10 min. Filling of a neuron was considered to be complete after robust and homogeneous fluorescence had built up in all its dendrites, especially in the thin distal branches far away from the cell body and in the dendritic spines that occasionally decorate such dendrites. We injected/filled between 3 and 10 neurons in each slice, maintaining a separation between cells of 400–500 μ m. In total, we LY-injected 95 retrogradely labeled neurons.

Slices containing intracellularly injected neurons were transferred to cold PB-buffered 4% formaldehyde, post-fixed overnight and transferred to 20% glycerin and 2% DMSO (Merck, Germany) in PB (Rosene, Roy, & Davis, 1986). Next, they were frozen on dry ice and resectioned

at 40 μ m, parked in ice-cold PB at pH 7.6 and subsequently incubated overnight at room temperature in a cocktail of two primary antibodies in TBS-TX: anti-LY raised in rabbit (1:1,000; Incstar) mixed with anti-TH raised in goat (1:1,000, Santa Cruz). After rinsing in TBS, we continued incubation for 1 hr with a cocktail of donkey-anti-rabbit IgG-Alexa Fluor 488, donkey-anti goat IgG-Alexa Fluor 633 and, to detect the transported BDA, streptavidin-Alexa Fluor 546. After final rinsing, the sections were mounted on gelatinized slides, thoroughly dried, dipped in toluene, coverslipped in Entellan, and stored at -20°C in a freezer. We documented all sections by taking images with a digital camera mounted on a standard fluorescence microscope.

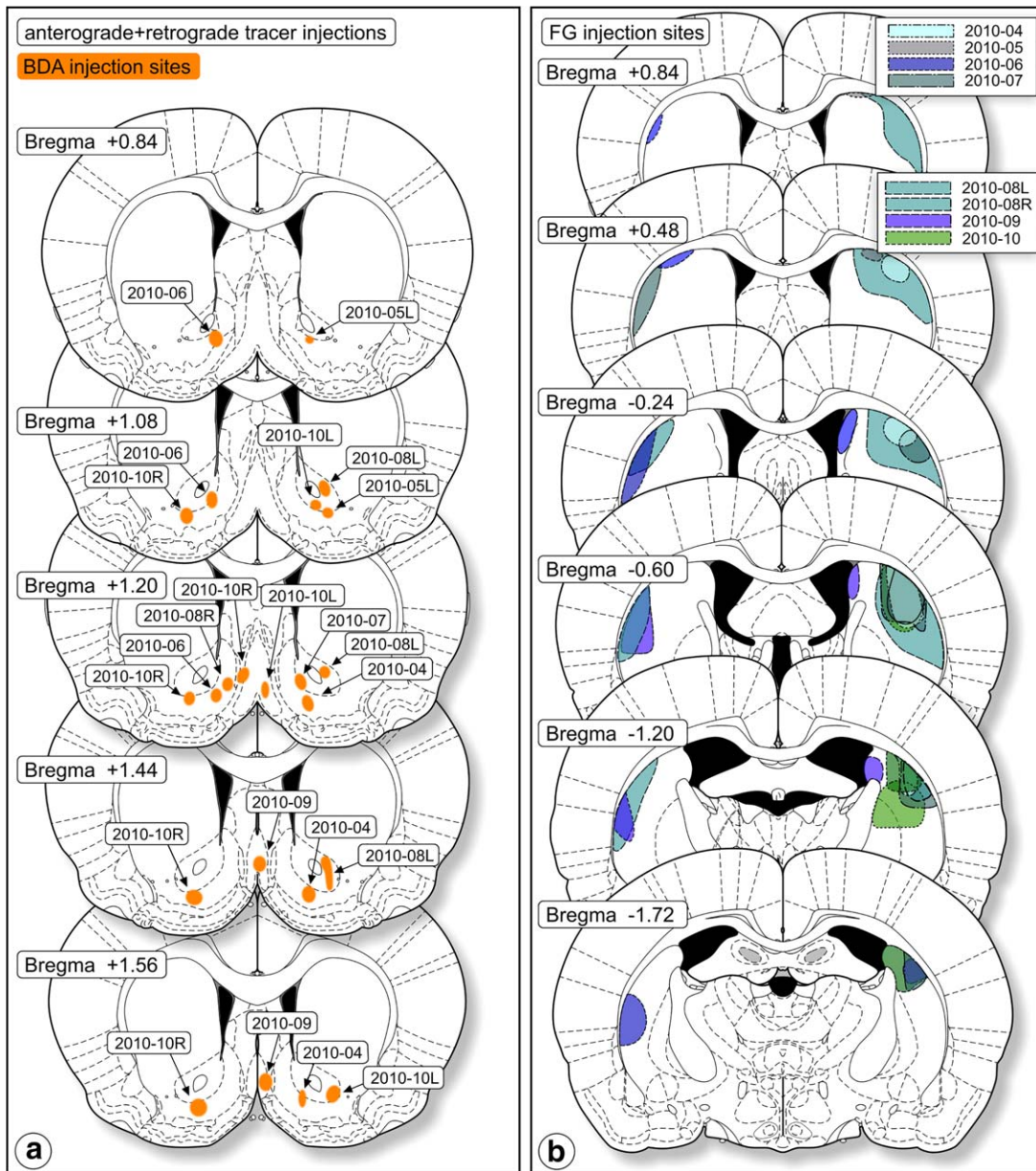


FIGURE 5 Tracer injection sites in the combined anterograde-retrograde study (Group C). (a) Anterograde tracer injection sites. (b) Injection sites of the retrograde tracer, FluoroGold (FG). These cases were the basis for the intracellular injection study [Color figure can be viewed at wileyonlinelibrary.com]

2.2.5 | Mounting, coverslipping

Sections were mounted on glass slides from 50 mM Tris-HCl (pH 7.6) containing 0.2% gelatin (Oxoid LTD, Hampshire, UK) and dried. Most mounted sections were dehydrated via an ascending ethanol series to xylene and coverslipped using Entellan (Merck). Slides to be used in the confocal laser scanning part of the study were thoroughly air-dried, placed for 10 s in toluene, and coverslipped directly with Entellan.

2.3 | Multifluorescence confocal laser scanning microscopy

Images were acquired with a Leica TCS-SP2 AOBS confocal instrument (CLSM; Leica Microsystems, Heidelberg, Germany) equipped with an Ar/

Kr laser (488 nm) and with HeNe lasers (543 and 633 nm). We configured three separate channels on the instrument: "green" (488 nm laser excitation; 493–535 nm emission bandpass filtering), "red" (543 nm excitation; 555–625 nm emission bandpass filtering), and "infrared" (633 nm excitation; 643 nm emission longpass filtering). A *channel* is a balanced series of specific settings of the instrument with the purpose to detect emission from a specific fluorochrome and nothing else: excitation laser wavelength, emission wavelength, dichroic mirror, emission filter range, and detector settings (see details in Wouterlood, 2006). Sections were visually inspected at low magnification. Prior to high-magnification image acquisition, we imaged regions with TH immunopositive staining (VTA, SN) at low magnification (10x) to prepare mosaic maps for accurate image sample documentation purposes.

TABLE 1 Coordinates of injection spots, that is, centers of gravity of staining determined in sections, after immunohistochemical processing and normalized to coordinates of the rat brain atlas of Paxinos and Watson (2005)

A. Dorsal striatum injections						
		bregma	lat	Z (from pia)		
2012-001	PHA-L	2.2	2.2	4.2		
2012-001	BDA	-0.1	3.2	3.3		
2012-002	PHA-L	1.0	3.1	4.2		
2012-002	BDA	-1.4	3.8	4.0		
2012-004	BDA	-1.1	3.8	3.2		
2012-005	PHA-L	2.5	2.5	3.8		
2012-005	BDA	1.0	3.3	4.4		
2016-006	BDA	1.0	3.3	4.4		
B. Ventral striatum injections						
		bregma	lat	X (from pia)		
79	BDA	1.2	0.8	6.3		
104	BDA	1.9	1.4	5.6		
105	BDA	1.9	1.2	6.0		
106	BDA	1.7	1.2	5.4		
107	BDA	1.9	1.4	6.2		
171	BDA	1.9	0.8	6.4		
1009L	BDA	2.5	0.8	5.0		
1009R	BDA	2.2	0.7	5.0		
1032	BDA	1.7	0.9	5.1		
2012-004	PHA-L	0.4	2.8	6.3		
90468 (EM)	PHA-L	1.7	0.9	5.0		
C. Anterograde vStr + retrograde dStr + intracellular injection						
rat nr	bregma	BDA lat	Z (from pia)	bregma	FG lat	Z (from pia)
2010-04	1.7	1.8	7.4	-0.6	4.0	3.8
2010-05L	0.2	1.8	8.0	-1.3	4.5	3.8
2010-06	1.1	1.2	7.4	-1.3	4.5	4.6
2010-08L	0.7	1.4	8.0	-0.3	4.2	3.5
2010-09	1.6	0.3	6.3	-1.2	3.2	3.6
2010-10R	1.2	2.7	7.2	-1.3	4.0	4.5
2010-10L	1.0	1.8	7.6	-1.3	4.0	4.5

Note. BDA = biotinylated dextran amine; dStr = dorsal striatum; EM = ●●●; FG = FluoroGold; PHA-L = *Phaseolus vulgaris*-leucoagglutinin; vStr = ●●●.

2.3.1 | High magnification Z-scanning

"Samples" consisted of Z-stacks of images acquired in single or multiple channels at high magnification (63x glycerin immersion objective NA 1.30, zoom 8, pinhole 1.00 arbitrary units (Airy disk 100%), Z-increment 122 nm, approximately 40 images at 512 × 512 pixels, 8-bit sampling, each frame consisting of two averaged scans). Multiple channel acquisitions were always made in "sequential" mode. The position of each sample was carefully noted in the previously prepared mosaic map of the region.

Intracellularly injected neurons were localized in the confocal instrument and initially scanned rapidly at low magnification for making mosaic maps in which we marked all TH positive neurons in the region of interest including those that had been LY injected. As the maps had been constructed from information acquired in three independent channels, we had available at low magnification the LY injected cells, the BDA labeled afferents from Acb, and the distribution of TH. Next, individual LY labeled neurons and BDA labeled fibers were scanned in

all three channels with the high-resolution glycerin immersion objective lens (see above for scanning parameters; “sequential” mode).

2.4 | Confocal controls

Perfect calibration of our confocal instrument was considered extremely important when it comes to apposition and especially colocalization. To check instrument and laser calibration, we conducted in each imaging session a standard laser beam alignment check. Second, we ran at regular intervals a “live” calibration imaging session. For this purpose, we had incubated a few sections of rat mesencephalon containing BDA labeled fibers with a cocktail of the streptavidin conjugates Alexa Fluor 488, 546, and 633. These “live” calibration sections had been further processed identical to the experimental sections. We scanned them with channel configurations identical to those used for the experimental sections. In a well-tuned CLSM, imaging and 3D reconstruction reveals in these “live” calibration slides “by design” in overlay mode perfect signal “colocalization” in BDA labeled fibers and appendages (see Wouterlood, van Denderen, Blijleven, van Minnen, & Härtig, 1998). Image series acquired in sessions in which this essential control was unsatisfactory were discarded.

2.5 | Deconvolution, 3D-reconstruction, computer analysis, appositions, colocalization

Post-acquisition, all image files obtained at high magnification were processed with deconvolution software (Huygens Professional; SVI, Hilversum, The Netherlands, www.svi.nl). Deconvolution is necessary to extract at this extreme magnification in a statistically reliable way all relevant information from the image series (Wouterlood, 2006).

The 3D computer reconstruction requires the introduction of additional definitions related to spatial objects. A *bouton* is a term used here for a particular 3D object identified in image series of tracer-labeled fibers: a swelling of, or at the end of a fiber, with a diameter at least three times that of the fiber. Correlative light-electron microscopy of this type of swelling has shown that boutons must be considered as the light microscopic representations of axon terminals (Wouterlood & Groenewegen, 1985). The term *3D object* is reserved for three-dimensional structures identified in TH, VGAT, and/or LY image series. In TH- and LY images, 3D objects may represent fibers, dendrites, or perikarya “filled” with their respective fluorescence signal (e.g., Figure 2b). VGAT fluorescence signal always produced small 3D objects (representing aggregates of synaptic vesicles; e.g., Figure 3a–e).

Structures included in the image files were 3D-reconstructed by means of Amira™ visualization/modeling software (www.fei.com). Next, we searched for appositions between boutons of BDA-labeled striatonigral fibers and TH- or LY 3D objects. This requires a short explanation. Both boutons and 3D objects must be considered as aggregates of voxels extracted from several images in a Z image series. In the 8-bit image acquisition with our confocal instrument, pixels and their 3D derivatives (voxels) possess gray densities between 0 and 255. A voxel aggregate can be considered, like an onion, as a concentric series of skins wherein each skin contains voxels expressing identical

gray intensity values (isodensity skins). The outer skin, that is, the one that is visualized on screen in a 3D computer reconstruction, is called the “*isodensity envelope*.” The gray intensity value of this isodensity envelope is requested by the software as a threshold. As the selection of a particular threshold strongly determines the size, shape, and number of boutons and 3D objects distinguished by the software, objective and operator-independent, reproducible thresholding is of utmost importance (Wouterlood, 2006; Wouterlood & Beliën, 2014).

Appropriate isodensity envelope thresholds were calculated by processing the images with the public-domain program ImageJ (Rasband, 1997–), exploiting the plugin “3D object counter” (Fabrice Cordelières, Institut Curie, Orsay, France; see Bolte & Cordelières, 2006; procedure explained and discussed by Beliën and Wouterlood, 2012; Wouterlood & Beliën, 2014). Output consisted of thresholds defining the isodensity envelopes of boutons and 3D objects in their respective voxel matrices.

After threshold analysis, we conducted voxel matrix analysis (SCIL_ Image, TNO, Delft, The Netherlands). Scripts were used to instruct the software to determine whether conspicuous pairs of boutons and 3D objects fulfilled criteria to be counted as “contacts” (Beliën & Wouterlood, 2012). Briefly, structure A defined by its voxel matrix (matrix A, e.g., a bouton recorded in one channel of the confocal instrument) was considered to be in apposition with structure B (e.g., a dendrite recorded in a complementary channel in the confocal instrument and defined by voxel matrix B) if a minimum of 100 voxels overlap was reported by the software of the involved voxel matrices (A) and (B). This criterion is extensively discussed in Beliën and Wouterlood (2012) and in Wouterlood and Beliën (2014). Also for colocalization of fluorescence signal in structures, a quantitative criterion was applied: “colocalization” was reported by the software if a minimum of 200 voxels of the voxel matrix of a 3D object (e.g., a bouton) recorded in one channel in the confocal instrument coincided with the voxel matrix belonging to a 3D object scanned in a complementary channel (e.g., an aggregate of VGAT signal).

2.6 | Electron microscopy

Legacy electron microscopy material of rat mesencephalon was available from a previous experiment in which we had explored the experimental framework for the current single neuron intracellular injections (Wouterlood et al., 1992). This material (rat 90468; injection of PHA-L in Acb-c; injection spot plotted in Figure 3f included labeled terminal fibers and boutons in the VTA and medial substantia nigra following injection of the tracer in the core of nucleus accumbens. PHA-L detection, post-fixation, embedding, and sectioning are described in detail in the Wouterlood et al. (1992) paper.

2.7 | Electrophysiological studies

Male rats (body weight 275–300 g) were anesthetized with ketamine (100 mg/kg, i.p., supplemented every hour by 50 mg/kg i.m. injections; Imalgène 500, Rhone-Mérieux, Courbevoie, France) and fixed in a stereotaxic frame (Horsley-Clark; Unimécanique, Epinay-sur-Seine, France). Body temperature was monitored rectally and maintained at 36–38°C. Electrical stimulation of loci in the shell of nucleus accumbens

TABLE 2 Group A (rats with tracer injection in dorsal striatum loci): Numbers of appositions between boutons of tracer-labeled fibers and TH-immunopositive 3D objects

Contacts	SNc	SNr	RRF
Number of samples	16	111	5
Number of identified boutons (tracer image series)	2,099	14,036	1,132
Number of identified TH 3D objects (TH image series)	2,350	15,538	624
Number of boutons in apposition with a TH 3D object	355	1,526	440
Percentage of boutons in apposition with a TH 3D object	16.9%	10.9%	38.9%

Notes. In the BDA/PHA-L images, “boutons” usually represent swellings in/on the shafts or at the end of fibers; in the TH images, “3D objects” represent cell bodies and dendrites. The criterion for “apposition” is explained in the Materials and Methods section. RRF = retrorubral field; SNc = substantia nigra pars compacta; SNr = substantia nigra pars reticulata; TH = tyrosine hydroxylase. Results from three rats lumped.

(stereotaxic coordinates: Bregma: +1.4; L: 0.8; H: 7.4 mm from the cortical surface) and of the sensorimotor territory of the dorsal striatum (Bregma: +0.2; L: 3.8; H: 7.4 mm from the cortical surface) was achieved via stainless steel electrodes (diameter 400 μm ; tip-barrel distance 300 μm). Stimuli consisted of pulses of 0.6 ms width and 200–600 μA intensity delivered at a frequency of 1 Hz. Single-unit activity of VTA/SNc cells ipsilateral to the stimulation sites was recorded using glass micropipettes (6–10 M Ω) filled with a 600 mM NaCl solution containing 4% Pontamine Sky Blue. Action potentials were amplified and displayed on a memory oscilloscope. Spikes were separated from noise using a window discriminator and sampled online using a CED 1401 interface (Cambridge Electronics Design, Cambridge, UK) connected to a computer. Peristimulus time histograms were generated from 100 to 200 stimulation trials using 1 ms bins. The duration of the inhibitory response corresponds to the time during which no spike was observed. DA cells projecting to the dorsal striatum were identified using their classically defined electrophysiological characteristics: large duration spikes > 2 ms, low discharge frequency < 8 Hz, and latency of the antidromic spike evoked from stimulation of the dorsal striatum (Deniau, Hammond, Risz, & Feger, 1978; Guyenet & Aghajanian, 1978). The antidromic spikes were characterized by their fixed latency and their collision with spontaneous discharges within an appropriate time interval. In four of the subjects, the conduction time of the Acb-s-VTA/SNc pathway was determined from the latency of the antidromic spikes evoked in Acb-s cells following stimulation of the VTA/SNc (Bregma -5.2 ; L: 1.3; H: 7.9 from the cortical surface). At the end of each recording session, the tip of the stimulating electrode was marked by a deposit of iron (15 μA anodal, 20 s) and localized in histological sections through a ferrirocyanide reaction. The tip of the recording electrode was marked with Pontamine Sky Blue (8 μA cathodal, 20 min). Brains were removed and fixed in a 12% formalin solution, and the positions of electrodes were identified in 100 μm thick, serially cut frozen sections stained with safranin.

3 | RESULTS

3.1 | Anterograde neuroanatomical tracing

3.1.1 | Group A: Dorsal striatum injections

Anterogradely labeled fibers in these rats ($n = 5$) were seen running from the injection site in the dorsal caudate-putamen complex (injection sites

documented in Figure 1a) via the ventral caudate-putamen, ventral globus pallidus, and lateral hypothalamus to the VTA. From here, they innervated the SNr, with additional, less abundant labeling in the SNc. In total, we acquired from three of these rats 132 samples in the confocal instrument and analyzed appositions between boutons of tracer labeled fibers and TH-immunoreactive dendrites (Table 2). Most samples ($n = 111$) were obtained in SNr, with a few additional samples in SNc ($n = 16$) and in the retrorubral field (RRF; $n = 5$) in which the dopaminergic cell group A8 is located. The software identified 17,267 boutons in these samples in the tracer-associated image series and 18,512 3D objects in the TH-image series. Visually, the tracer labeled fibers in VTA and SN had distinguishable swellings (boutons) in terminal and en passant configurations (Figure 2a,c; indicated with arrows). A 3D reconstruction of the striking apposition seen in the boxed area in the merge Figure 2c is shown in Figure 2d. Thin fiber shafts connect the swellings (Figure 2a,c). While these connecting shafts were visually distinguishable, they were usually ignored by the 3D reconstruction software and the voxel matrix analysis software because the computer algorithms considered their lower fluorescence intensity relative to boutons below threshold. Boutons seen in the confocal images had diameters of approximately 1 μm which is in the same range as axon terminals seen in electron microscopy (Figure 2e). The 3D objects recorded in TH image series were larger than the boutons reconstructed in the tracing images, which is consistent with presence of the TH-signal in cell bodies and dendrites (Figure 2b,c). VGAT imaging (Figure 3a–e) recorded punctate staining (blue signal in Figure 3a), that in 3D reconstruction appeared as small 3D objects (Figure 3b). As the size of individual synaptic vesicles was sub resolution in our confocal instrument, we interpreted the punctate VGAT staining as representing small clusters of synaptic vesicles carrying the transporter. Expression of VGAT signal inside a BDA labeled bouton (“colocalization”; bouton b5* in Figure 3a) is shown in 3D reconstruction in Figure 3b. Also in pairs of single frames taken from the image series of this bouton, colocalization of signal is clearly present (illustrated in Figure 3c–e).

In all three regions tested: SNc, SNr, and RRF, boutons were identified in apposition with TH 3D objects. In SNc, the percentage of appositions (16.9%) was higher than in SNr (10.9%) whereas in RRF a much higher percentage was seen (38.9%). Appositions nearly always occurred between a labeled axon terminal and a TH immunopositive

TABLE 3 Group B (rats with tracer injection in ventral striatum loci): Injection of tracer in nucleus accumbens (Acb)

Tracer injection site in:	Acb-c	Acb-c	Acb-c	Total	Acb-s	Acb-s	Acb-s	Acb-s	Acb-s	TOTAL	ENTIRE
Rat case	104	105	106	Acb-c	79	107	171	1009	1032	Acb-s	Acb
SNC (lumped)											
Number of samples	67	9	52	128	12	28	25	55	102	222	350
Number of boutons	34,987	6,258	19,451	60,696	5,128	13,364	10,439	24,521	42,679	96,131	156,827
Number of boutons in contact with TH 3D object	11,916	4,582	10,944	27,442	1,108	7,574	4,419	8,631	9,344	31,076	58,518
% of boutons in contact with TH 3D object	34.1	73.2	56.3	45.2	21.6	56.7	42.3	35.2	21.9	32.3	37.3
SNr (lumped)											
Number of samples	56		63	119		24	4	47	8	83	202
Number of boutons	27,374		50,230	77,604		14,076	1,114	18,287	4,248	37,725	115,329
Number of boutons in contact with TH 3D object	11,787		24,442	36,229		7,545	816	8,407	2,640	19,408	55,637
% of boutons in contact with TH 3D object	43.1		48.7	46.7		53.6	73.2	46.0	62.1	51.4	48.2

Notes. "Common" analysis of double immunofluorescence stained mesencephalon sections. Appositions between boutons and TH-3D objects. The criterion for "apposition" is explained in the Materials and Methods section. Acb-c = core of Acb; Acb-s = shell of Acb; SNC = substantia nigra pars compacta; SNr = substantia nigra pars reticulata; TH = tyrosine hydroxylase.

dendritic shaft (e.g., Figures 2–3, and 7j,k). The TH immunopositive neurons had few dendritic spines anyway.

3.1.2 | Observations of "woolly" fiber terminals

In several Group A rats, we noted in VTA conspicuous configurations of tracer-labeled fibers, usually a combination of two labeled fibers that

TABLE 4 Group B (rats with tracer injection in the shell (Acb-s) or core (Acb-c) of nucleus accumbens)

ROIs (punches)	Acb-c	Acb-s
SNC		
Number of boutons analyzed	186	400
Number of boutons in contact with TH 3D object	170	178
% of boutons in contact with TH 3D object	91.4	44.5
SNr		
Number of boutons analyzed	301	522
Number of boutons in contact with TH 3D object	196	116
% of boutons in contact with TH 3D object	65.1	22.2
RRF		
Number of boutons analyzed	74	89
Number of boutons in contact with TH 3D object	45	63
% of boutons in contact with TH 3D object	60.8	70.8

Notes. "Punch" analysis of double stained sections (tracer + TH). Conditions as explained in Table 3. Acb-c = core of Acb; Acb-s = shell of Acb; SNC = substantia nigra pars compacta; SNr = substantia nigra pars reticulata; TH = tyrosine hydroxylase.

over short segments formed tight, irregular meshes wrapping in a semi-spiralling way around a cylindrical optically "empty" tissue volume approximately 1 μm in diameter and a few microns long. These meshes included fiber segments and boutons (Figure 1d–g). The diameters and volumes of the involved cylindrical volumes had dimensions suitable for dendrites. However, although TH-immunofluorescent dendrites in all cases occurred abundantly in the immediate vicinity of woolly fiber configurations we never observed any TH-immunofluorescent dendrite filling of such a configuration (Figure 1d–g).

A wrapped fiber configuration suggests intimate contact of the involved fiber with the structure or structures inside the volume around which wrapping occurs. We assume that the involved structures are dendrites belonging to local, TH immunonegative neurons. Presumed dendrites are indicated with dashed lines in the 3D reconstruction in Figure 1g. The morphologies of the terminal fiber wraps comply with the description of "woolly" fiber terminal configurations reported by Haber and Nauta (1983), in rhesus and macaque monkeys identified as endings of fibers of striatal origin (Haber, Wolfe, & Groenewegen, 1990; Parent, Charara, & Pinault, 1995).

3.1.3 | Group B: Ventral striatum injections

In eight animals belonging to this group, the injections appeared successful as judged from injection spots consisting of a compact cluster of labeled neuronal cell bodies with their dendrites radiating out, the presence of traceable, labeled fibers, projections to the mesencephalon, local collateral fibers, and terminal labeling. The injection spots in Group B rats (documented in Figure 3f) were small (diameter <200 μm). They occurred at various positions in nucleus accumbens (Acb) in locations that based on the calbindin staining pattern were considered shell (Acb-s; cases 79, 107, 171, 1009, and 1032) or core region (Acb-

TABLE 5 Group 3 rats: intracellularly injected, retrogradely labeled cells in VTA and SN

Area	Position relative to IP nucleus	Sagittal position in VTA or SN	Cell body phenotype	
VTA (n = 14)	Rostral to IP (n = 14)	Medial (n = 1)	Bipolar	
		Lateral (n = 13)	Bipolar (n = 3)	
			Triangular (n = 1)	
			Multipolar (n = 5)	
			Pear (n = 4)	
VTA (n = 6)	Next and caudal to IP (n = 6)	Medial (n = 1)	Pear	
		Lateral (n = 5)	Bipolar (n = 1)	
			Triangular (n = 2)	
			Pear (n = 2)	
Total VTA: n = 20				
SNc (n = 27)	Rostral to IP (n = 16)	Medial (n = 10)	Bipolar (n = 40)	
			Multipolar (n = 4)	
			Pear (n = 2)	
		Intermediate (n = 6)	Bipolar (n = 2)	
			Multipolar (n = 4)	
		Lateral	No cells labeled/injected	
		Next and caudal to IP (n = 11)	Medial (n = 7)	Bipolar (n = 2)
				Triangular (n = 1)
		Multipolar (n = 2)		
		Pear (n = 2)		
		Intermediate (n = 1)	Pear	
		Lateral (n = 3)	Triangular (n = 1)	
			Multipolar (n = 1)	
			Pear (n = 1)	
SNr (n = 3)	Rostral to IP (n = 1)	Intermediate	Pear	
	Next and caudal to IP (n = 2)	Medial (n = 1)	Bipolar	
			Intermediate (n = 1)	Multipolar
Total SN: n = 30				

Notes. The position of the cells is given along the antero-posterior axis relative to the interpeduncular nucleus (N). For the substantia nigra (SN), we list the location of injected retrogradely labeled according to three sagittal zones: medial, intermediate, and lateral. IP = interpeduncular nucleus ; VTA = ventral tegmental area.

c; cases 104, 105, and 106). Micrographs of injection spots of experiments 105 and 79, respectively, are shown in Figure 4a,c.

Labeled fibers from the Acb injection sites traveled caudally into the ventral pallidum and further via the ventrolateral hypothalamus to the mesencephalon where the majority of the arriving fibers ended among populations of TH immunopositive neurons in SNc and SNr, and to a minor extent in the VTA and RRF. Injection spots in the rostral lateral Acb-c resulted in labeled fibers predominantly in rostromedial parts of the SN, whereas in cases with injection spots located caudally and medially in Acb-c, that is, diagonally opposite the rostromedial Acb-c injections, innervation was seen predominantly of caudomedial SN regions. When the injection site was centered in Acb-s, more fibers

were seen in the VTA than in cases where the injection site was located in Acb-c. In several cases (e.g., in case 1032), we were able to follow labeled fibers all the way from the injection site to the SN (Figure 4b).

3.1.4 | “Common” and “punch” analysis of labeled striatomesencephalic fibers

Analysis of images acquired from mesencephalic loci in Group A rats was performed at two levels, “common analysis” and “punch analysis.” In “common analysis,” a large number of samples was screened in their entirety by software for the occurrence of boutons of fibers in the tracer-associated channel and, in the associated TH imaging channel, of 3D objects (cell bodies, dendrites). Next, the results were computer

processed to detect appositions of fiber boutons and TH-3D objects. On a separate set of samples, we conducted “punch analysis,” that is, in such samples we digitally selected regions of interest (ROIs) with promising fiber boutons and TH dendrites and we manually cropped the images series such to include only the ROIs. Next, we subjected these “punched-out” ROIs to data analysis. The advantage of the latter approach was that the analysis was done very efficiently with (visually) morphologically identified labeled boutons, at the expense of introducing bias.

The result of the common analysis is provided in Table 3. Image acquisition included 552 samples. In both, SNc and SNr numerous appositions were identified between (tracer-labeled) boutons and TH 3D objects. In SNc, 45.2% of all boutons seen in the samples after injection of tracer in Acb-c were in apposition with TH 3D objects. In SNr, this apposition ratio was of the same order (44.5%). For boutons associated with Acb-s injections, the ratio of apposing boutons versus all boutons was lower (32.3%) in SNc but in SNr of the same order of magnitude (45.1%) as following injection of tracer in Acb-c.

In “punch” samples, we analyzed single boutons. This type of analysis was performed on material from five rats: injection of tracer in Acb-c (rats 105 and 106) and injection of tracer in Acb-s (rats 107, 2010-09, and 2010-10) (Table 4).

The Acb-c series included samples acquired in SNc, SNr, and RRF. The tracer had been deposited in the caudomedial core of Acb. In total, we analyzed from these cases 561 labeled boutons selected from ROIs. Of the boutons in SNc 91.4%, in SNr 65.1%, and in RRF 60.8% was found to be in apposition with TH positive structures.

Both in SNc and in SNr, we noted in their ventromedial and ventral portions a higher number of tracer-labeled boutons than in dorsolateral portions, that is that most tracer labeled projection fibers were seen in ventral parts of the SN. The number of boutons in apposition with TH-immunofluorescent structures was approximately twice as high in the ventral SNr and SNc compared with more dorsal levels of SNc and SNr, leading us to suspect a higher preference for Acb-c fibers to appose TH-immunopositive structures in the ventromedial SN compared with dorsolateral levels.

In the Acb-s series, we acquired samples in SNc, SNr, and RRF. The total number of analyzed “punched out” boutons in these samples was 1,374. In SNc, 44.5% of the boutons was in apposition with TH 3D objects whereas this percentage was 22.2 in SNr and 70.8 in RRF.

In Group B material, we found in several samples VGAT expression inside boutons of BDA labeled fibers, similar to that in Group A (the latter illustrated in Figure 3a–e).

3.1.5 | Electron microscopy

In the electron microscope, we observed PHA-L labeled boutons in contact with the shafts of small to medium sized dendrites in SN. The example of a labeled axon terminal shown in Figure 2e was obtained in the medial SNr bordering VTA. Tracer-filled boutons were laden with synaptic vesicles. Synaptic junctions in these contacts invariably were of the symmetrical type.

3.1.6 | Group C: Double neuroanatomical tracing

Plots of injection sites of anterograde and retrograde tracer in the subjects of this group are summarized in Figure 5. FG injections centered in the dorsolateral part of the dorsal striatum (sensorimotor territory) produced retrograde labeling of neuronal cell bodies in the sensorimotor cortex as well as in the mesencephalon. Retrograde labeling in the sensorimotor cortex has been reported earlier (Deniau & Thierry, 1997; Deniau et al., 1996) and was used by us to validate the location of the FG injection sites. Retrogradely labeled neurons in the ventral mesencephalon were observed over the entire mediolateral extent of the SNc, at various rostrocaudal levels as well as more medially in the dorsolateral part of the VTA. There was a clear difference in the strength of the labeling of neurons in different parts of the VTA/SNc complex. In the dorsal tier of the SNc, densely labeled neurons were intermingled with more weakly labeled cells, while most retrogradely labeled cells which we noted in the most medial aspects of the SNc and in the VTA were only lightly labeled. Extensive overlap between anterograde and retrograde labeling was present in the lateral part of the VTA and dorsal part of the medial SNc. Appositions of boutons of anterogradely filled, BDA containing fibers with retrogradely labeled, FG-containing neuronal cell bodies or dendrites were observed frequently in the VTA. In more lateral parts of SNc, the anterogradely labeled fibers were mostly segregated from the retrogradely labeled nigrostriatal neurons, with these cells occupying a ventral position with respect to the labeled fibers.

3.1.7 | Double neuroanatomical tracing combined with intracellular injection

Successful combinations of tracer injections and intracellular injections were achieved in seven subjects: rats 2010-04 through 2010-10. Injection of the anterograde tracer had been aimed at Acb-s; this aim had been successfully achieved in all rats except 2010-08 where the injection spot occurred in Acb-c (see Figure 5a). Injection sites of the retrograde tracer occurred in the dorsolateral striatum (documented in Figure 5b). In total, we documented penetration into and intracellular filling with LY of 95 mesencephalic, retrogradely FG labeled neurons. However, during the resectioning of the thick slices we lost material. Ultimately, we recovered 50 LY-injected neurons (i.e., cells with an intact cell body and at least one LY-filled dendrite, numbers, and characteristics described in Table 5: 30 cells in SN and 20 cells in VTA). The positions of the successfully retrogradely labeled, LY injected, and recovered cells are presented in Figure 6. In addition to complete neurons, we recovered 96 sections of LY-filled dendrites of which the parent cell body had been damaged during LY injection or had been lost during processing. In all cases, anterogradely labeled fibers were present in the VTA (i.e., Acb-s injections) and the adjacent middle and intermediate parts of the substantia nigra (Acb-c and Acb-s injections). Anterogradely labeled fibers occurred as strings of rounded and fusiform boutons on fibers in en passant and terminal positions. In case 2010-04, we observed “woolly” fiber configurations of anterogradely labeled fibers in VTA. Similar to “woolly” fibers present in rats with dorsal striatum injections also these “woolly” fiber configurations never wrapped around TH-immunopositive

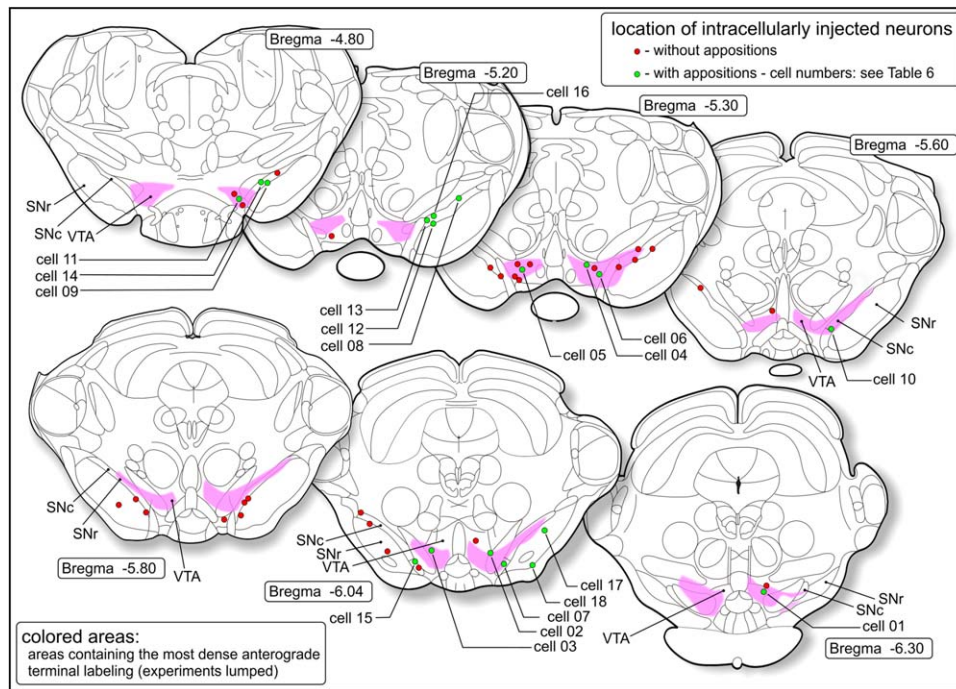


FIGURE 6 Combined anterograde-retrograde tracing/intracellular injection study (Group C). Locations of retrogradely labeled neurons in the ventral tegmental area (VTA), substantia nigra pars compacta (SNc), or substantia nigra pars reticulata (SNr) that were successfully filled with Lucifer yellow. The cells indicated with green circles had appositions with fibers labeled with anterograde tracer. Numbers of these cells correspond with those in Table 6. The colored zones correspond with the areas where the highest densities were present of labeled striatomesencephalic fibers. Around these areas labeled fibers occur much sparser [Color figure can be viewed at wileyonlinelibrary.com]

dendrites but instead around unstained space, obviously occupied by dendrites.

3.1.8 | Cell morphology of intracellularly injected neurons

LY-filled cell bodies showed a heterogeneity of shapes including small globular cell bodies with multipolar dendritic configuration, bipolar cells with slender, fusiform cell bodies, pear-shaped cell bodies, and big cells with triangular cell bodies and with a thick dendrite originating from each corner of their cell bodies. Big bipolar cells occurred in the VTA with dendritic trunks emanating from opposite corners of their perikaryon, while other big cell bodies had multipolar dendrite configurations. The main types are illustrated in Figure 7a–d and categorized in Table 6. In the CLSM channel associated with TH-immunofluorescence, these cells appeared without exception to be moderately TH-immunopositive (illustrated in Figure 7e–g).

3.1.9 | Intracellularly injected neurons apposed by striatal efferents

As the intracellular injections had been blind conducted prior to the immunohistochemical processing, many of the injected neurons listed above appeared to be apposition-negative in the sense that their cell bodies were located outside the area hosting anterogradely labeled fibers. We report here only on apposition-positive neurons, that is, retrogradely FG labeled and intracellularly LY-injected neurons whose cell bodies or dendrites were observed to be in apposition with anterogradely labeled fibers of ventral striatal origin (summarized in Table 6). As the slices with intracellularly injected neurons had been resectioned

into thinner sections, we had to reconstruct neurons by combining the thinner sections. A total of 19 apposition-positive cells were recovered in this way, that is, cell bodies with part of their dendritic tree. In addition to such “complete” neurons, we found 23 fragments of apposition-positive LY-filled dendrites in SNr which we could not trace back to a particular cell body. The location and characteristics of these neurons and dendrites are also summarized in Table 6. The longest fragment of an apposition-positive dendrite is illustrated in Figure 8a. Six of the apposition-positive neurons were identified in the VTA. These neurons had cell bodies with bipolar, triangular, or multipolar shapes/dendrite arrangements. They received sparse innervation by the striatal efferent fibers. Appositions of boutons were scattered over the cell bodies and dendrites. The apposition-positive neurons in SNc ($n = 10$) expressed bipolar and multipolar shapes; their dendrites extended into SNr where appositions with boutons of anterogradely labeled fibers occurred. An example of a SNc apposition-positive neuron is provided in Figure 7, panels H–K (neuron ID 2010-08-L10-1-01, see below). Cells in SNr with appositions of boutons of labeled striatal afferents were scarce; we recovered only one such neuron (2010-08-R07-8-05), possessing three appositions on its cell body and one on a dendrite. One apposition-positive neuron was found embedded in the cerebral peduncle, ventral to SNc.

3.1.10 | Typical case: Cell 2010-08-L10-1-01

The cell body of this neuron was located in the ventral most portion of SNc, and its dendrites extended into SNr (Figure 7h–k). Its perikaryon was big (short diameter of approximately 15 μm) and

TABLE 6 Group 3 rats: characteristics of retrogradely labeled, LY injected, recovered neurons that had appositions with boutons of anterogradely, BDA labeled striatonigral fibers

Cell nr (Figure 6)	Identified neuron ID	Location	Cell body	Specialty	TH pos	nr of appositions on		
						Perikaryon	Dendrites	
01	2010-04-R06-1-01	VTA	Lateral	Triangular	y	2	4	
02	2010-05-L07-9-02	VTA	Lateral	Bipolar	y	0	1	
03	2010-05-R06-4-01	VTA	Medial	Bipolar	y	2	3	
04	2010-05-R07-9-01	VTA	Lateral	Triangular	y	3	2	
05	2010-05-R09-0-03	VTA		Multipolar	y	1	1	
06	2010-08-R09-3-01	VTA	Medial	Multipolar	?	0	1	
07	2010-05-R07-9-02	SNC	Medial		y	0	2	
08	2010-08-L07-3-01	SNC	Lateral		y	2	3	
09	2010-08-L07-3-04	SNC	Lateral		y	1	0	
10	2010-05-L07-9-04	SNC	Medial	Bipolar	y	1	0	
11	2010-08-L10-1-01	SNC	Medial		y	0	5	
12	2010-08-R07-8-03	SNC		Multipolar	y	0	4	
13	2010-08-R09-3-03	SNC		Multipolar	n	2	1	
14	2010-08-R11-5-01	SNC		Bipolar	Pear	y	2	1
15	2010-08-R11-5-07	SNC		Multipolar	?	0	2	
16	2010-08-R11-5-08	SNC		Triangular	?	2	1	
17	2010-08-R07-8-05	SNr		Multipolar	Pear	y	3	1
18	2010-08-R07-8-06	Peduncle		Multipolar	?	2	0	
19	2010-08-L09-1-03	?	?		Pear	y	1	0
	Dendrite fragments slice	Dendrites with contacts			TH pos		nr of contacts	
	2010-07-L10-9	1			y		1	
	2010-07-L12-1	6			y		7	
	2010-07-L12-9	6			y		8	
	2010-07-L12-3	3			y		5	
	2010-07-L12-8	7			y		9	

Notes. Same for LY-filled fragments of neurons not traceable to cell body (cell body lost during immunoprocessing) (dendrites) (rat 2010-07). TH immunopositivity was in several cases not tested (indicated with "?" in the TH pos column). The locations of these neurons are indicated in Figure 6.

BDA = biotinylated dextran amine; LY = Lucifer Yellow; SNC = substantia nigra pars compacta; SNr = substantia nigra pars reticulata; TH = tyrosine hydroxylase; VTA = ventral tegmental area.

it was morphologically classified as "pear" shaped. The principal dendritic trunk pointed toward the SNr and it bifurcated after 30 μ m into secondary branches designated " α " and " β ." Branch α further branched into α_1 , α_2 , and into sub-branches $\alpha_{1.1}$ and $\alpha_{1.2}$. These dendrites traversed at a more or less perpendicular orientation the bundle of parallel oriented BDA labeled fibers arriving from the ventral striatum (Acb-c injection site). In total, we observed on dendrites $\alpha_{1.2}$ and β five sites where boutons of BDA labeled fibers were in apposition with the LY-filled dendrites (indicated with arrowheads in Figure 7i). The site of which the position is indicated in Figure 7i with a rectangular dashed-line box is shown at high magnification in Figure 7h-j, while Figure 7k

is the 3D reconstruction of this apposition. Visible here are two boutons of the BDA labeled fiber, each forming an apposition on the dendrite, and each with boutons on an opposite side of the dendrite, a configuration resembling an earmuff (EMC; Figure 7j; 3D reconstruction Figure 7k). "Earmuff" appositions were seen only in association with distal dendrites, and they occurred frequently. The most striking example of such an apposition was observed on a LY-filled dendrite in case 2010-09-L13, process 079 (Figure 8b,c). In several cases, the parent fiber of the involved labeled bouton ran for a short distance immediately close and parallel to the LY-filled dendrite (e.g., Figure 8b,c and 8d,e).

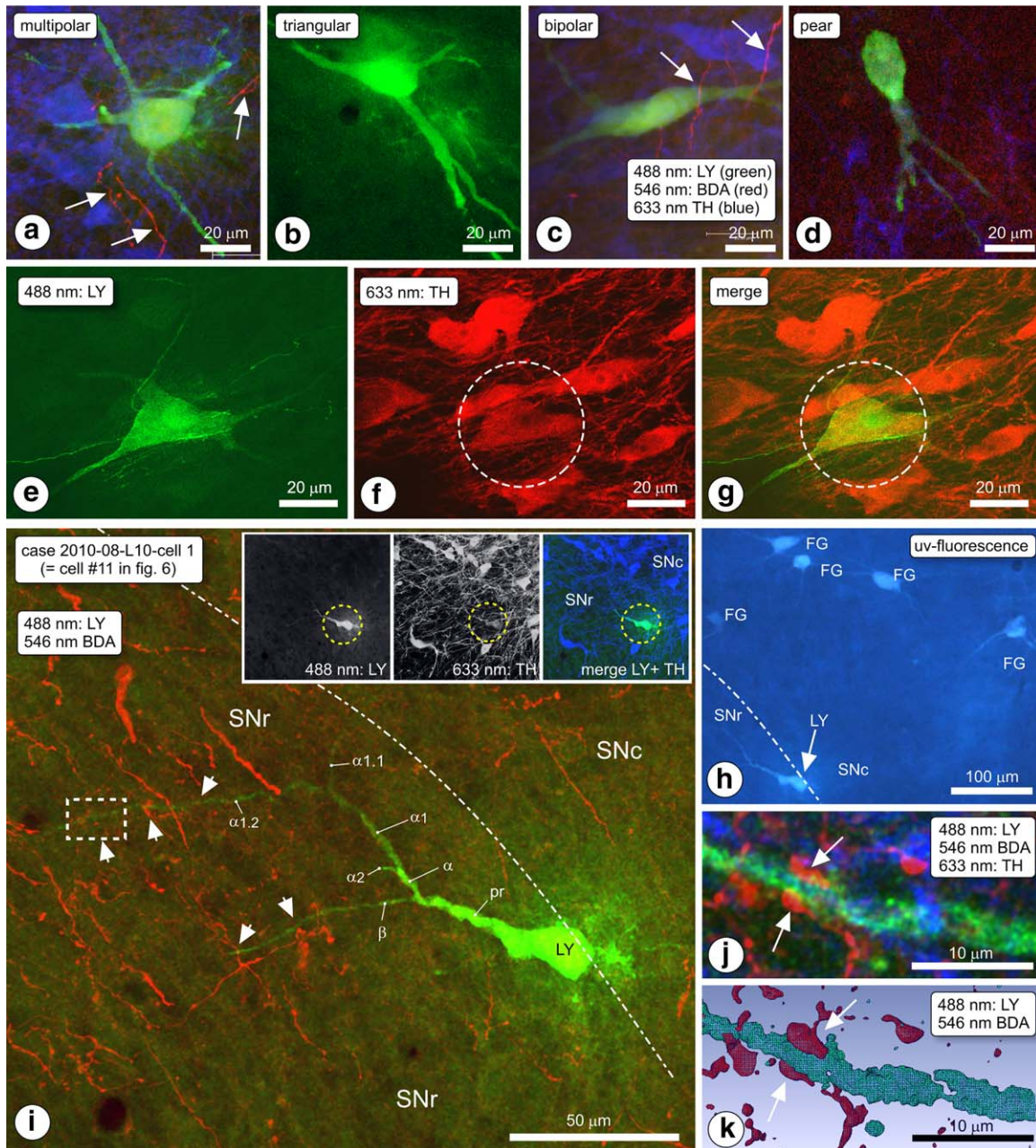


FIGURE 7 (a–d) Morphological phenotypes of intracellularly Lucifer yellow (LY)-injected, retrogradely labeled SN/VTA neurons. (a) Multipolar, (b) triangular. (c) Bipolar, (d) pear-shaped. Arrows indicate biotinylated dextran amine (BDA) labeled fibers (red). (e–g) Expression of tyrosine hydroxylase (TH) in an LY-injected retrogradely labeled SN neuron, visualized by two-channel CLSM. (e) LY channel, (f) TH-channel, (g) merged image. (h–k) Example of a LY-injected, retrogradely labeled neuron. Rat 2010-008, slice L10, cell #1. (h) Inspection of the area in a fluorescence microscope revealed a LY injected, FG labeled neuron (LY). (i) In the CLSM, the neuron was scanned first at low magnification such that the spatial relationships between the cell body (LY) and dendrites (green; arrowheads indicate appositions) and the anterogradely labeled striatal fibers (red) became visible in the merge image. The TH-channel is omitted here because the location of the neuron at the edge between substantia nigra pars compacta (SNc) and substantia nigra pars reticulata (SNr) produced a massive TH-associated signal overwhelming other colors in the merge image (all three channels visible in the inset). The dashed-line boxed area indicated in panel (i) was Z-scanned at high magnification, shown here in projection image (j) and in 3D reconstruction (k). Arrows indicate an apposition between boutons of BDA labeled fibers and identified dendrite α 1.2, in SNr, approximately 100 μ m away from the perikaryon. The appositions form an “earmuff” contact [Color figure can be viewed at wileyonlinelibrary.com]

3.2 | Neurophysiology

In 14 rats, the responses evoked by electrical stimulation of the shell of the Acb were investigated in a grand total of 152 cells antidromically driven from the orofacial sensorimotor territory of the dorsal striatum

(Deniau & Thierry, 1997; Deniau et al., 1996). These cells were characterized as dopaminergic based on their long duration action potential (>2 ms), relatively low spontaneous activity (<8 Hz), and mean latency of antidromic activation (11.7 ± 0.2 ms). The cells antidromically driven

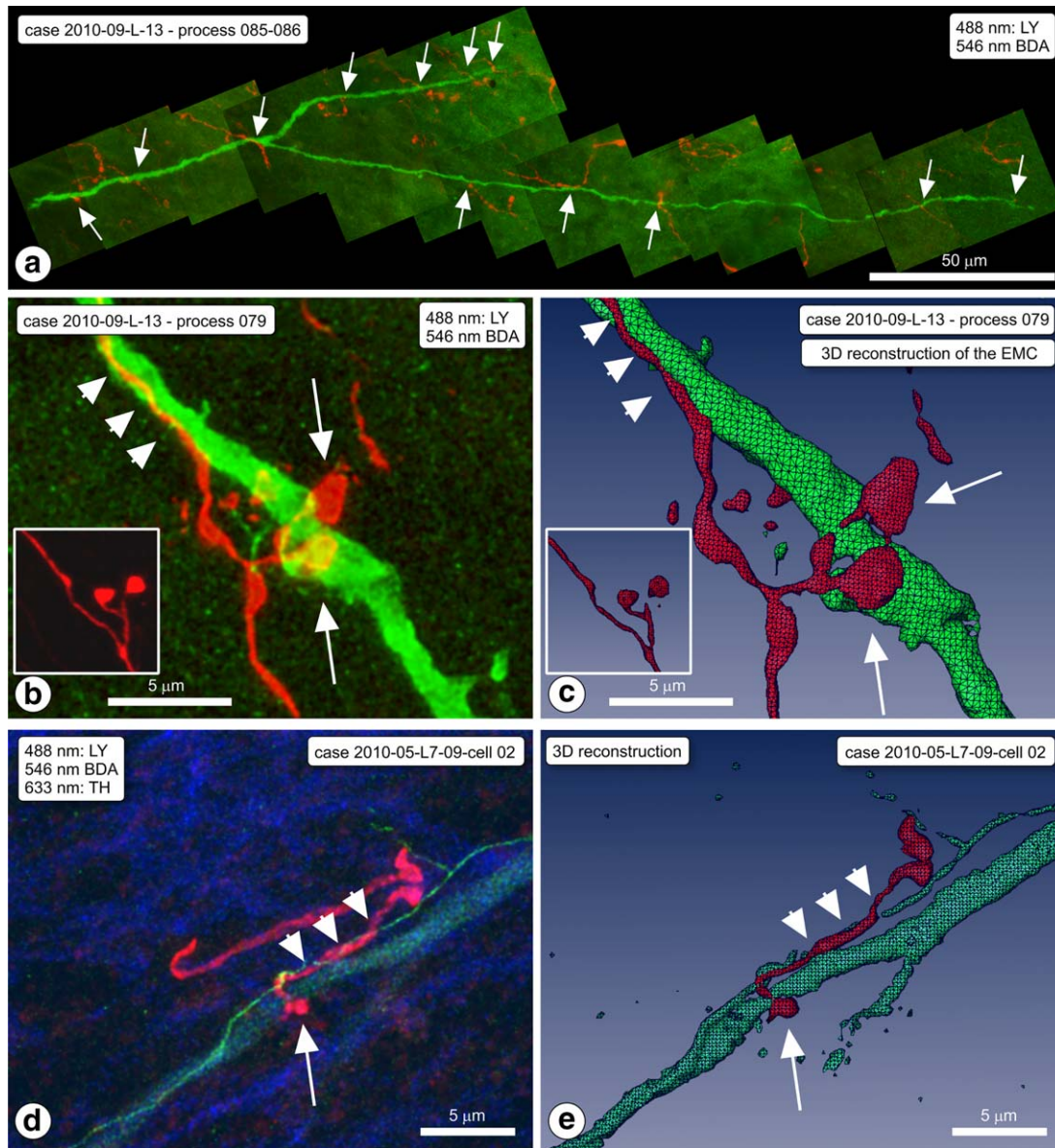


FIGURE 8 Examples of appositions of boutons of ventral striatal afferent fibers in SN on dendrites of intracellularly Lucifer yellow (LY)-injected, dorsal striatum (dStr) projecting neurons. (a) Case 2010-009-L-12 on process 085/086 (cell body not recovered). Montage of projection images covering a LY labeled dendrite (green) and the striatal fibers in the area, with appositions (arrows). (b) Same rat; LY dendrite (process nr 079). High magnification projection image of one of the appositions, a typical “earmuff” apposition (EMC). BDA = red. Inset: EMC seen in animal nr. 106. (c) 3D computer reconstruction of the EMC (arrows) shown in frame (b). Note that the BDA-labeled fiber runs for a while alongside the dendrite (arrowheads). The inset is the 3D reconstruction of the inset of frame (b). (d) Another example of an “earmuff” apposition. Case 2010-005. (e) 3D computer reconstruction of this EMC (arrows) of the sample shown in frame (d) [Color figure can be viewed at wileyonlinelibrary.com]

from the dorsal striatum were located throughout most of the medio-lateral extent of the SNc and the lateral part of the VTA. In addition, 15 other cells were antidromically driven from the shell; these cells were located more medially in the VTA.

Electrical stimulation of the shell induced an inhibitory response in 69 of the 152 cells antidromically driven from the dorsal striatum. The evoked response had a mean latency of 17.8 ± 0.9 ms and a mean duration of 38.8 ± 3.0 ms (Figure 9a,b). As shown in Figure 9c, these cells were located in the medial SNc and lateral part of the VTA, mainly dorsally. In order to determine the conduction time of the shell-VTA/SNC pathway, the latency of the antidromic responses evoked in the shell (41 cells) by

stimulation of the VTA/SNC complex was determined. The mean latency of the antidromic responses was 16.7 ± 0.2 ms (range: 13–20 ms).

4 | DISCUSSION

In this study, we collected evidence along independent anatomical and electrophysiological lines of approach that neurons in the shell area of nucleus accumbens (Acb-s), in the ventral striatum, exert an inhibitory influence on dopaminergic neurons that are located in the lateral portion of the VTA and medial SN and that project to the sensorimotor

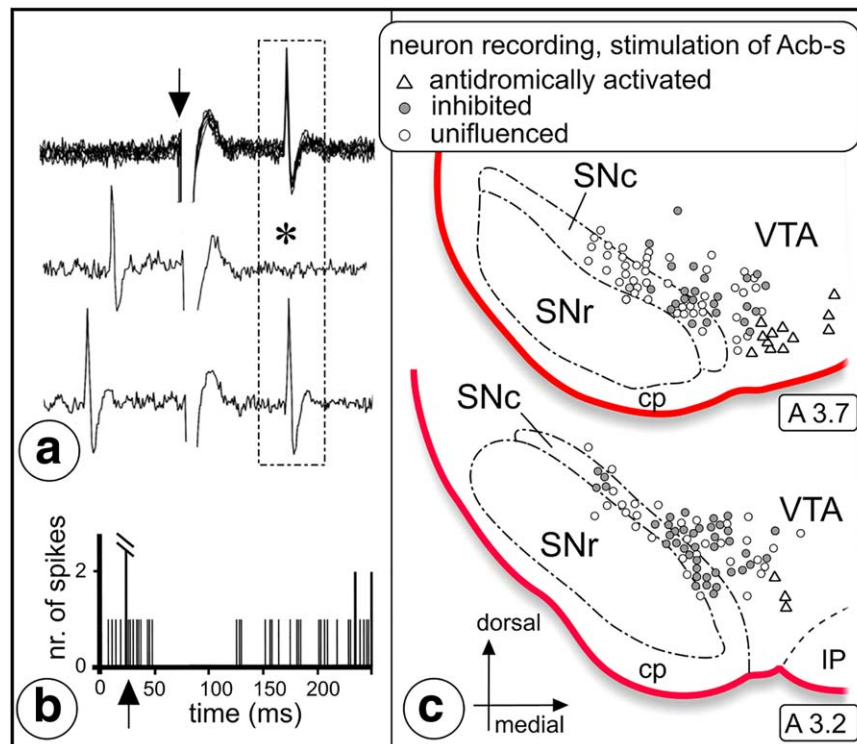


FIGURE 9 Inhibitory effect evoked by stimulation of Acb-s in neurophysiologically identified dopaminergic nigrostriatal neurons projecting to the sensorimotor dorsal striatum (dStr). (a) Neurophysiological identification of a nigrostriatal neuron by antidromic activation following an electrical stimulation applied in the orofacial sensorimotor territory of the ipsilateral dStr. Upper trace: fixed latency (17 ms) of the antidromic response. Arrow indicates time of application of the stimulation. Middle and lower traces: collision test. Note the lack of the antidromic response (asterisk) when the striatal stimulation is preceded by a spontaneous discharge of the neuron upon an appropriate time interval. (b) Inhibitory response of this nigrostriatal neuron to stimulation of Acb-s. Arrow indicates the time of application of the stimulation. (c) Distribution within VTA/SNC of the neurons antidromically activated from dStr and either inhibited by stimulation of Acb-s (filled circles) or uninfluenced by Acb-s stimulation (open circles). Triangles indicate the location of neurons antidromically activated by stimulation of Acb-s. Abbreviations: A = anterior, cp = cerebral peduncle; SNc = substantia nigra pars compacta; SNr = substantia nigra pars reticulata; VTA = ventral tegmental area [Color figure can be viewed at wileyonlinelibrary.com]

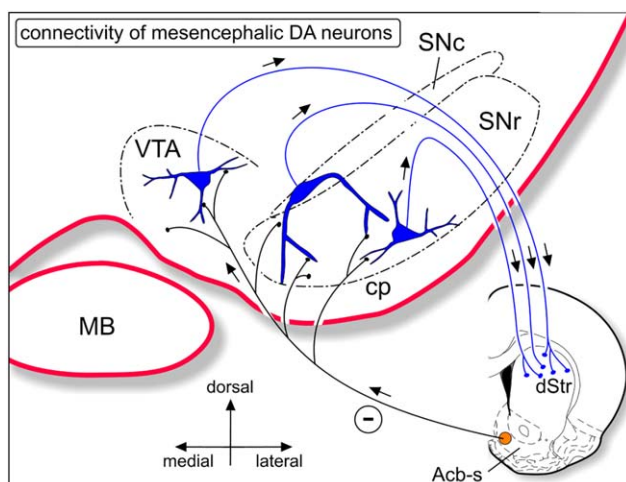


FIGURE 10 Simplified scheme of the identified striato-mesencephalic-dopaminergic-dStr connectivity. Neurons in Acb-s inhibit dopaminergic neurons in VTA, SNr, and SNc that project to the sensorimotor region of the dorsolateral striatum. Dopaminergic neurons indicated in blue. dStr = dorsal striatum; MB = mammillary body; SNc = substantia nigra pars compacta; SNr = substantia nigra pars reticulata; VTA = ventral tegmental area [Color figure can be viewed at wileyonlinelibrary.com]

territory of the dorsal striatum (dStr; connectivity schematized in Figure 10). We will first briefly discuss the methodological approaches. Subsequently, our data will be discussed in the context of existing knowledge of the link between the ventral striatum and the dorsal striatum via the dopaminergic system. Finally, we will provide some functional considerations.

4.1 | Methodological approaches: Advances and limitations

Anatomical experiments included single anterograde tracing and more complex, combined tracing, and immunohistochemical experiments. Injections with an anterograde tracer in the dorsal (Group A) and ventral (Group B) striatum were extended with neurochemical phenotyping of recipient neurons (see Wouterlood et al., 2014) using antibodies against TH. With an additional immunofluorescence layer using antibodies against vesicular GABA transporter (VGAT), we noted colocalization of neuroanatomical tracer and VGAT fluorescence signal, thus indicating that these projection fibers belong to GABAergic striatal neurons. In the more complex experiments of Group C, we combined anterograde and retrograde neuroanatomical tracing, intracellular

injection of LY in slices of fixed brain, and TH immunofluorescence phenotyping. In parallel to the neuroanatomical experiments, neurophysiological experiments were conducted to establish the electrophysiological characteristics of these connections.

When a bouton on a fiber is observed to be in physical apposition with a potential postsynaptic structure such as a TH immunofluorescent cell body or dendrite, this does not prove per se that there is synaptic contact and information exchange between the two. However, an axon terminal needs to physically appose a dendrite (as can be appreciated in electron microscopy: Figure 2e) or cell body to provide a substrate platform for the synapse that performs the information exchange. We consider the appositions that we observed in confocal laser scanning microscopy to represent such platforms. The analysis of the striatomesencephalic boutons in SNc, SNr, and RRF belonging to dorsal striatum projections (Table 2) revealed boutons in apposition with TH expressing dendrites in the order of magnitude of 11% (SNr), 17% (SNc), and 39% (RRF). Fibers from ventral striatum projections (Tables 3 and 4) had three times more appositions with TH expressing dendrites, in the order of magnitude of 40–45%, both in SNr and SNc.

Even if only a fraction of these appositions form true synaptic contacts, there still is considerable connectivity. Most appositions were of the casual type that is formed between a bouton present on a fiber while it crosses a dendrite. A type of apposition that suggests a more intimate contact was the “ earmuff ” type of apposition type illustrated in Figures 7j,k and 8b–e. Finally, the electrophysiological experiments complemented the anatomical observations in showing that dopaminergic neurons in VTA and medial SNc that were orthodromically identified as projecting to the dorsal striatum could in a large percentage be inhibited by stimulation of the medial part of the ventral striatum. Taken together, we conclude that in our study a significant proportion of the close appositions observed in the VTA-substantia nigra region must represent inhibitory synaptic contacts onto dopaminergic cells and dendrites. In addition, the literature supplies studies providing evidence that neurotransmission in striatonigral connectivity is overwhelmingly GABAergic (for instance: Ferraguti et al., 1990; reviews by Galvan & Wichmann, 2007; Gerfen, 2004; Tepper & Lee, 2007). Our current observation of VGAT immunofluorescence signal inside BDA-labeled boutons (Figure 3a–e) complements the above reports.

4.2 | Striatal inputs and outputs at the level of mesencephalic dopamine neurons

Recent reviews emphasize the complex structural and functional relationships of inputs and outputs at the level of the ventral mesencephalic dopaminergic neurons, in particular the VTA (Chuhma et al., 2011; Morales & Margolis, 2017; Sesack & Grace, 2010; Xia et al., 2011). Consequently, it is important to firmly establish the synaptic and neurophysiological characteristics of the ventral striatal and dorsal striatal efferents at the level of the VTA and substantia nigra as performed in our study and compare these results with the existing literature. Thus, in morphological terms the axon terminals in our electron microscopic material of striatomesencephalic projections, their postsynaptic dendrites, and the involved synapses show great similarity with

the early observations made by Wassef, Berod, and Sotelo (1981), Somogyi et al. (1981), and Bolam and Smith (1990) in SN and VTA after lesions or injections of an anterograde tracer in dorsal striatal loci: endings on smooth shafts of dendrites, expressing symmetrical synapses. By contrast, corticomesecephalic (glutamatergic) innervation forms axon terminals in VTA that display asymmetrical synapses (Carr & Sesack, 2000; Sesack & Pickel, 1992); such synapses are supposed to be excitatory.

Both VTA and SN are composed of a mixture of dopaminergic, GABAergic and even glutamatergic cellular elements (reviews: Morales & Margolis, 2017; Sesack & Grace, 2010). Within VTA, dopaminergic neurons form 60–65% of the total population, with the remaining fraction being predominantly GABAergic (Sesack & Grace, 2010). Dopaminergic neurons in SN are concentrated in the pars compacta, but ventrally located neurons in SNc extend their dendrites deep into SNr. Furthermore, whereas SNr primarily consists of GABAergic neurons, there are also groups of dopaminergic neurons embedded in its ventral part. Thus, in order to arrive at the conclusion that direct appositions exist between Acb-s afferent fibers and dopaminergic neurons in VTA and SN it was necessary to precisely characterize the neurons and their dendrites as projecting to the dStr and being dopaminergic. To do so, we injected retrogradely labeled neurons from the dStr with LY to identify the dendrites of such scattered neurons in VTA and substantia nigra. We followed up with TH-immunofluorescence to verify that the injected cells were indeed dopaminergic. Dendrites of several of these identified cells received appositions from identified Acb-s efferents (Table 6). Interestingly, appositions occurred either on cell bodies of LY injected neurons or on secondary dendrites, with the latter appositions being tens to hundreds of microns away from the LY injected cell body (e.g., cell 2010-08-L10-1-01, see Figure 7h–k). Here, also the “ earmuff ” type of apposition occurred. We have a strong impression that, in particular, neurons in the medial SNc possess dendrites that may “ stick ” into adjacent portions of VTA and SNr where dense innervation occurs of fibers of ventral striatal origin. We consider the identification by LY injection of dendrites of dopaminergic, dStr projecting neurons crucial here since boutons of ventral striatum efferents also appose TH-negative, most likely GABAergic neurons in SN. In the Group B experiments with tracer injected in Acb, the percentage of boutons in SNc not apposing TH 3D objects (and therefore likely apposing GABAergic neurons) was approximately 65% in SNc and 51% in SNr (Table 3).

The actual picture of the cells of origin of TH expressing dendrites in VTA and SNr is even more complex because dopaminergic neurons with their cell bodies in SNc have been reported to extend long dendrites into SNr and VTA (Björklund & Lindvall, 1975). LY intracellular injection into retrogradely labeled SNc neurons made it possible to follow such dendrites specifically. An example of an SNc dopaminergic neuron whose dendrites extend far into SNr to receive appositions here by striatal efferents, including one of the “ earmuff ” type, is provided in Figure 7.

Whereas we concentrated in this study on the VTA-substantia nigra complex, we also observed appositions between striatal efferents and dopaminergic elements in the RRF. In a very limited number of samples (5) in RRF, of the total of 1,132 boutons, 39% was apposed to

TH-expressing dendrites. Inherently, the number of boutons counted in the RRF was much lower than that in the VTA and SN (Table 2). We did not inject retrogradely labeled neurons in the RRF intracellularly with LY, precluding any definite conclusions as to VStr-to-DStr connections via dopaminergic RRF neurons. To firmly establish such a connection, further experiments are necessary. Whereas the results of other studies would also be in support of such connections, neurons in the RRF (A8 dopaminergic cell group) have a much wider distribution of their axons in the forebrain than only the striatum. In particular cell groups that together form the extended amygdala appear to be a primary target of RRF fibers (for review see: Yetnikoff, Lavezzi, Reichard, & Zahm, 2014)

Figure 10 summarizes our interpretation of the above-discussed connectivity. The number of appositions on dopaminergic neurons can be described as modest and the appositions are spatially separated on the dendrites. "Earmuff" appositions (Figure 7j,k and 7b,e) suggest very specific relationships. We noted this type of configuration in several of the cases. Appositions of this type may form the morphological substrate producing the inhibitory postsynaptic currents observed by Xia et al. (2011) in VTA dopaminergic neurons following optogenetic stimulation of fibers arriving in VTA from Acb.

Altogether our data support the existence of a direct functional link between the limbic ventral striatum and the sensorimotor dorsolateral striatum, wherein dopaminergic SN and VTA neurons form the "linking" cellular elements in the mesencephalon. Further confirmation of a functional link between Acb-s and the VTA/SNC neurons that project to rather extensive parts of the dorsal striatum, is derived from the finding that an important portion of electrophysiologically identified DA neurons antidromically activated from the ventrolateral, orofacial striatal territory presented an inhibitory response to Acb-s stimulation. In agreement with the anatomical data, these cells were mainly located in the medial SNC and lateral VTA (Figure 9) suggesting that Acb-s exerts an inhibitory influence preferentially on the "distal" subpopulation of nigrostriatal projection neurons as defined by Maurin et al. (1999). The inhibitory responses evoked by Acb-s stimulation on these dStr projecting neurons are likely monosynaptic since their latency is consistent with the conduction time of the Acb shell-VTA/SNC pathway (present study). In addition, it is known that neurons in Acb-s with efferent connections are GABAergic (Ferraguti et al., 1990). Finally, VTA/SNC cells antidromically driven from dStr and inhibited by Acb-s stimulation in previous studies exhibited electrophysiological characteristics of dopaminergic neurons (Deniau et al., 1978; Guyenet & Aghajanian, 1978). Even though our injections of retrograde tracers were directed at the dorsolateral, sensorimotor-related part of the dStr, and the electrodes providing the antidromic stimulation in the electrophysiological experiments were located in the orofacial, ventrolateral part of the dStr, we consider the results of these experiments as supporting our conclusion that vStr projections have an inhibitory influence of dopaminergic projections to the dStr. As discussed below, this must be considered as an "open component" of the various existing striatal-mesencephalic-striatal loops.

Although the present anatomical and electrophysiological study was focused onto the neurons of the VTA/SNC innervating the

orofacial and sensorimotor territories of dStr, it is likely that a similar link exists between Acb-s and "distal" subpopulations of dopaminergic SN neurons innervating other, for example, "cognitive" districts of the dStr since these subpopulations share the spatial distribution in the lateral VTA and medial part of SNC (Maurin et al., 1999).

4.3 | Spiraling or direct projections from ventral to dorsal striatum via the dopaminergic system?

Our present results confirm and extend previous neuroanatomical studies in demonstrating that ventral striatal efferents influence dopaminergic neurons in VTA and SNC that in turn project to more dorsal striatal areas, including the dorsolateral and ventrolateral, sensorimotor and orofacial related parts of the dStr (rat: Nauta et al., 1978; monkey: Haber et al., 2000; Ikemoto, 2007). Thus, there appears to be a two-neuron pathway between Acb-s and these sensorimotor-related areas in the caudate-putamen in rats. However, the fact that the projections from Acb-s reach, among others, the "distal" subpopulation of dopaminergic neurons in the lateral VTA and medial SNC suggests that Acb-s may influence the dopaminergic innervation of more extensive parts of the dStr as well as the core of the Acb as this "distal" subpopulation consists of a mixture of neurons that reaches widespread parts of the striatum (Maurin et al., 1999).

In primates the organization of striato-nigro-striatal pathways has been interpreted as a spiraling system (Haber et al., 2000) implying that the influence from ventral-to-dorsal striatum via the ventral mesencephalon shifts gradually, that is, striatal projections target small groups of dopaminergic neurons in SNC that each provide a feedback projection to the striatal area of origin and in addition project to a striatal region located more dorsally. This provides for a step-by-step mediolateral shift in the substantia nigra and leads to the possibility that functionally different striatal regions influence each other in a transition from motivational via cognitive to sensorimotor-related functions (Haber et al., 2000). Whether in rats such a gradual shift also exists in the organization of the projections between different parts of the striatum and the dopaminergic cell groups cannot directly be concluded from the results of the present study. Based on light microscopic tracing experiments, Ikemoto (2007) suggested that such a step-by-step hierarchical organization exists from the medial olfactory tubercle via the Acb-s and Acb-c to the dorsal striatum (see his figure 13). In more functional terms, Ikeda, Saigusa, Kamei, Koshikawa, and Cools (2013) reported a spiraling circuitry from different striatal regions via the dopaminergic system, running from the Acb-s via, subsequently, the Acb-c and the ventrolateral part of the dStr to its dorsolateral part. Considering the results of Maurin et al. (1999) that terminal fields of various, functionally different striatal regions might overlap with "distal" subpopulations of nigral neurons projecting to the dStr, such an arrangement might be present in rats. However, the precise organization of such stepwise organized striatal-mesencephalic-striatal loops with "open" and "closed" aspects still needs to be determined. Nevertheless, our results are not in contradiction with such arrangements but provide evidence that next to a stepwise organization from ventral to dorsal, there is also a more direct route.

It is important to add a few notes here. The direct projections from the vStr to the dopaminergic neurons imply an inhibitory action on the DA neurons. In very simple terms, in case this would be the only connection in the circuitry, physiological activity in the vStr projections would simply lead to a decrease of the DA levels in the dorsal striatum and, thus, to a diminished cognitive and motor output of the striatum. That would seem to be in contradiction with the original ideas of Nauta, Mogenson, and colleagues of a mechanism from “motivation to action” (Mogenson et al., 1980; Nauta et al., 1978). The results of the study by Ikeda et al. (2013) seems to confirm the inhibitory actions in the spiraling model: stimulation of the Acb-s leads to a lower dopamine release in the Acb-c and, in a serial action of these inhibitory next to disinhibitory dopaminergic guided loops, to a higher dopamine release in the dorsolateral striatum. However, true as this may be, the direct projections from vStr neurons to DA neurons in VTA that project to the dStr, form part of a much more complex circuitry. Thus, the vStr projects to the ventral pallidum, which in turn sends direct projections to the dopaminergic neurons in the ventral mesencephalon (Tripathi et al., 2010; Tripathi, Prensa, & Mengual, 2013). Whether the projections of interconnected vStr and ventral pallidal neurons converge on the same DA neurons in VTA of SNc is at present unknown. The activity of DA neurons in VTA is dependent on a variety of excitatory (mostly brainstem and cerebral cortex) and inhibitory inputs (mostly from the basal ganglia). However, the influence of the basal ganglia is more complex than a simple inhibitory influence, for example, as the projections from vStr via ventral pallidum may ultimately be disinhibitory (reviewed by Sesack & Grace, 2010). Furthermore, with respect to the projections from vStr to non-DA neurons and dendrites within the substantia nigra-VTA complex, there might also be an indirect, disinhibitory influence from these vStr neurons on the DA neurons (Bocklisch et al., 2013), also since most of the GABAergic nigral and VTA neurons have local axon collaterals or serve as interneurons (Gerfen & Bolam, 2017).

Although not explicitly studied as yet, the results of Maurin et al. (1999) together with the present results might provide for the following possible organization. Maurin et al. (1999) suggest the existence of a dual projection system between the striatum and the dopaminergic cell groups in VTA and substantia nigra. First, there is the subpopulation of “proximal” neurons that provides in principle closed loops between specific parts of the striatum and particular DA cell groups in SNc. However, it might very well be possible that this circuitry is not as “closed” as is suggested but that, like in primates, there is an “open” component in these loops which forms the basis for a spiral-like, rather specific organization (compare Haber et al., 2000; Ikeda et al., 2013). Second, the direct projections from the vStr to the “distal” subpopulation of DA neurons in the lateral VTA and medial SNc have a much more widespread influence on the striatum and this population is inhibited by the vStr. Physiological activity in the vStr projections to these neurons might lead to a general decrease of dopamine levels in extensive striatal areas preparing for more specific, focused increases in DA levels brought about by the indirect, disinhibitory actions, for example, via the ventral pallidum or GABAergic neurons in SNr, on the DA neurons participating in the spirals.

5 | CONCLUDING REMARKS

From the above considerations, it is clear that our results indicate the existence of a two-neuron inhibitory projection from the shell of the Acb via dopaminergic neurons to the dorsolateral striatum. The strength of these projections is difficult to establish with the present experimental approach but seems in quantitative terms modest at most. It should be kept in mind that this two-neuron pathway forms part of a much more complex circuitry that may connect the ventral and dorsal striatum via the dopaminergic system, as discussed above. Our anatomical and physiological results do not allow direct conclusions as to the functional significance of these projections. Nevertheless, multiple recent studies (cited below) indicate that the direct inhibitory projections from the vStr onto DA neurons projecting to the dStr play a role in some behavioral or dysfunctional aspects in which the vStr and the DA system have been implicated. Thus, the proposed role for the vStr, in particular Acb, in action selection, be it appetitively or aversively motivated, fits well with organization of inputs and outputs of this region and its relationships with the DA system (recent review: Floresco, 2015; see also Groenewegen et al., 2016; Menegas et al., 2015). This role of the vStr in action selection may be exerted in on-going behavior but may also be important over a longer time. Behavioral studies on the consolidation of “normal” motor skills show the importance of the successive striatal region- and pathway-specific involvement in this process (Yin et al., 2009). Likewise, the presently described circuitry involving the vStr, DA neurons, and the orofacial part of the dStr might play a role in feeding behavior, as extensively studied by Ann Kelley and colleagues (e.g. Kelley, Baldo, & Pratt, 2005; Richard, Castro, Difeliceantonio, Robinson, & Berridge, 2013). Furthermore, the role of the vStr and the spiraling DA projections to the dStr has received specific attention in studies concerning the development of maladaptive behaviors in the context of drug addiction, and disorders of impulsivity and compulsivity. The hypothesis behind this is that stimulus-reward driven behavior, represented in the Acb-s, via instrumental learning behavior mediated through the Acb-c, over time leads to habitual behaviors for which parts of the dStr are crucial. In particular, in the context of studies of the development of addictive behaviors, the shift of striatal involvement from ventromedial to dorsolateral and the role of dopamine has been established quite clearly. In an initial study by Belin and Everitt (2008), using intrastriatal disconnection procedures, it was shown that interactions between ventral and dorsal areas in the striatum, mediated by dopamine, are crucial in the development of habitual cocaine-seeking. These findings have been confirmed and extended in the context of addiction studies in more recent years, not only behaviorally but also using neurophysiological and neurochemical approaches (Adermark et al., 2016; Burton, Nakamura, & Roesch, 2015; Coffey et al., 2015; Keramati & Gutkin, 2013; Sadoris, Wang, Sugam, & Carelli, 2016; Willuhn, Burgeno, Everitt, & Phillips, 2012; Willuhn, Burgeno, Groblewski, & Phillips, 2014). Recent studies also show “spiraling” between the Acb-s and Acb-c in the context of behavioral actions and the transition from impulse control disorders into compulsive disorders (e.g., Besson et al., 2010; Diergaarde et al., 2008).

In conclusion, behavioral and neurophysiological studies underpin the importance of the “spiraling” pathways between the vStr and dStr via dopaminergic neurons in the ventral mesencephalon as established in the present and previous studies (Haber et al., 2000; Ikemoto, 2007; Nauta et al., 1978). In essence, this means that the Acb-s, implicated primarily in action selection and emotional-motivational behavior, via a subpopulation of mesencephalic dopaminergic neurons, is able to influence the dorsal striatum which is primarily involved in executive and procedural behaviors. In this way, dopaminergic neurons provide a link through which motivational and emotional states can influence motor outcomes.

ACKNOWLEDGMENTS

The authors thank Yvonne Galis-de Graaf and Lucienne Baks-te Bulte for expert histochemical assistance and Bogdan Kolomiets for his contribution to the neurophysiological experiments. Nico Blijleven and Riichi Kajiwara are acknowledged for putting much effort and time in writing the ImageJ scripts that form the basis of objective threshold analysis.

CONFLICT OF INTEREST

No conflicts of interest exist for any of the authors of this study.

AUTHOR CONTRIBUTIONS

FGW, YCvD and HJG, as principal authors, directed research and wrote the paper. AE, MD, GH, AM, TJS and JAMB were involved in imaging, data collection, computer analysis and for developing innovative ideas. JS-K, A-MT and J-MD's are responsible for the conceptual framework, reference, discussion and consultation.

ORCID

Floris G. Wouterlood  <http://orcid.org/0000-0002-5442-5384>

REFERENCES

- Adermark, L., Morud, J., Lotfi, A., Danielsson, K., Ulenius, L., Söderpalm, B., & Ericson, M. (2016). Temporal rewiring of striatal circuits initiated by nicotine. *Neuropsychopharmacology*, *41*(13), 3051–3059.
- Alexander, G. E., & Crutcher, M. D. (1990). Functional architecture of basal ganglia circuits: Neural substrates of parallel processing. *Trends in Neurosciences*, *13*(7), 266–271.
- Belien, J. A. M., & Wouterlood, F. G. (2012). Confocal laser scanning: Of instrument, computer processing and men. In F. G. Wouterlood (Ed.), *Cellular imaging techniques for neuroscience and beyond* (pp. 2–34). Cambridge, MA: Academic Press.
- Belin, B., & Everitt, B. J. (2008). Cocaine seeking habits depend upon dopamine-dependent serial connectivity linking the ventral with the dorsal striatum. *Neuron*, *57*(3), 432–441.
- Besson, M., Belin, D., McNamara, R., Theobald, D. E., Castel, A., Beckett, V. L., ... Dalley, J. W. (2010). Dissociable control of impulsivity in rats by dopamine d2/3 receptors in the core and shell subregions of the nucleus accumbens. *Neuropsychopharmacology*, *35*(2), 560–569.
- Björklund, A., & Lindvall, O. (1975). Dopamine in dendrites of substantia nigra neurons: Suggestions for a role in dendritic terminals. *Brain Research*, *83*(3), 531–537.
- Bocklisch, C., Pascoli, V., Wong, J. C., House, D. R., Yvon, C., de Roo, M., ... Lüscher, C. (2013). Cocaine disinhibits dopamine neurons by potentiation of GABA transmission in the ventral tegmental area. *Science*, *341*(6153), 1521–1525.
- Bolam, J. P., & Smith, Y. (1990). The GABA and substance P input to dopaminergic neurones in the substantia nigra of the rat. *Brain Research*, *529*(1–2), 57–78.
- Bolte, S., & Cordelières, P. (2006). A guided tour into subcellular colocalization analysis in light microscopy. *Journal of Microscopy*, *224*(3), 213–232.
- Buhl, E. H., Schwedtfeger, W. K., Germroth, P., & Singer, W. (1989). Combining retrograde tracing, intracellular injection, anterograde degeneration and electron microscopy to reveal synaptic links. *Journal of Neuroscience Methods*, *29*(3), 241–250.
- Burton, A. C., Nakamura, K., & Roesch, M. R. (2015). From ventral-medial to dorsal-lateral striatum: Neural correlates of reward-guided decision-making. *Neurobiology of Learning and Memory*, *117*, 51–59.
- Calzavara, R., Maily, P., & Haber, S. N. (2007). Relationship between the corticostriatal terminals from areas 9 and 46, and those from area 8A, dorsal and rostral premotor cortex and area 24c: An anatomical substrate for cognition to action. *The European Journal of Neuroscience*, *26*(7), 2005–2024.
- Carr, D. B., & Sesack, S. R. (2000). Projections from the rat prefrontal cortex to the ventral tegmental area: Target specificity in the synaptic associations with mesoaccumbens and mesocortical neurons. *The Journal of Neuroscience*, *20*(10), 3864–3873.
- Chaudhry, F. A., Reimer, R. J., Bellocchio, E. E., Danbolt, N. C., Osen, K. K., Edwards, R. H., & Storm-Mathisen, J. (1998). The vesicular GABA transporter, VGAT, localizes to synaptic vesicles in sets of glycinergic as well as GABAergic neurons. *The Journal of Neuroscience*, *18*(23), 9733–9750.
- Chuhma, N., Tanaka, K. F., Hen, R., & Rayport, S. (2011). Functional connectome of the striatal medium spiny neuron. *The Journal of Neuroscience*, *31*(4), 1183–1192.
- Coffey, K. R., Barker, D. J., Gayliard, N., Kulik, J. M., Pawlak, A. P., Stamos, J. P., & West, M. O. (2015). Electrophysiological evidence of alterations to the nucleus accumbens and dorsolateral striatum during chronic cocaine self-administration. *The European Journal of Neuroscience*, *41*(12), 1538–1552.
- Deniau, J. M., Hammond, C., Risz, A., & Feger, J. (1978). Electrophysiological properties of identified output neurons of the rat substantia nigra (pars compacta and pars reticulata): Evidences for the existence of branched neurons. *Experimental Brain Research*, *32*(3), 409–422.
- Deniau, J. M., Menetrey, A., & Charpier, S. (1996). The lamellar organization of the rat substantia nigra pars reticulata: Segregated patterns of striatal afferents and relationship to the topography of corticostriatal projections. *Neuroscience*, *73*(3), 761–781.
- Deniau, J. M., & Thierry, A. M. (1997). Anatomical segregation of information processing in the rat substantia nigra pars reticulata. *Advances in Neurology*, *74*, 83–96.
- Diergaarde, L., Pattij, T., Poortvliet, I., Hogenboom, F., de Vries, W., Schoffeleers, A. N., & De Vries, T. J. (2008). Impulsive choice and impulsive action predict vulnerability to distinct stages of nicotine seeking in rats. *Biological Psychiatry*, *63*(3), 301–308.
- Einhorn, L. C., Johansen, P. A., & White, F. J. (1998). Electrophysiological effects of cocaine in the mesoaccumbens dopamine system: Studies in the ventral tegmental area. *The Journal of Neuroscience*, *8*, 100–112.

- Ferraguti, F., Zoli, M., Aronsson, M., Agnati, L. F., Goldstein, M., Filer, D., & Fuxe, K. (1990). Distribution of glutamic acid decarboxylase messenger RNA-containing nerve cell populations in the male rat brain. *Journal of Chemical Neuroanatomy*, 3, 377–396.
- Floresco, S. B. (2015). The nucleus accumbens: An interface between cognition, emotion, and action. *Annual Review of Psychology*, 66, 25–52.
- Galvan, A., & Wichmann, T. (2007). GABAergic circuits in the basal ganglia and movement disorders. *Progress in Brain Research*, 160, 287–312.
- Geisler, S., & Zahm, D. S. (2005). Afferents of the ventral tegmental area in the rat-anatomical substratum for integrative functions. *The Journal of Comparative Neurology*, 490(3), 270–294.
- Gerfen, C. R. (2004). Basal ganglia. In G. Paxinos (Ed.), *The rat nervous system* (3rd ed., pp. 455–508). New York: Elsevier Academic Press.
- Gerfen, C. R., & Bolam, J. P. (2017). The neuroanatomical organization of the basal ganglia. In H. Steiner & K. Y. Tseng (Eds.), *Handbook of basal ganglia structure and function* (2nd ed., pp. 3–32). Amsterdam, The Netherlands: Elsevier.
- Groenewegen, H. J., Voorn, P., & Scheel-Krüger, J. (2016). Limbic-basal ganglia circuits parallel and integrative aspects. In J.-J. Soghomonian (Ed.), *The basal ganglia, innovations in cognitive neuroscience* (pp. 11–45). Cham, Switzerland: Springer.
- Groenewegen, H. J., Wright, C. I., Beijer, A. V., & Voorn, P. (1999). Convergence and segregation of ventral striatal inputs and outputs. *Annals of the New York Academy of Sciences*, 877, 49–63.
- Guyenet, P. G., & Aghajanian, G. K. (1978). Antidromic identification of dopaminergic and other output neurons of the rat substantia nigra. *Brain Research*, 150(1), 69–84.
- Haber, S. N., Fudge, J. L., & McFarland, N. R. (2000). Striatonigrostriatal pathways in primates form an ascending spiral from the shell to the dorsolateral striatum. *The Journal of Neuroscience*, 20(6), 2369–2382.
- Haber, S. N., & Nauta, W. J. H. (1983). Ramifications of the globus pallidus in the rat as indicated by patterns of immunohistochemistry. *Neuroscience*, 9(2), 245–260.
- Haber, S. N., Wolfe, D. P., & Groenewegen, H. J. (1990). The relationship between ventral striatal efferent fibers and the distribution of peptide-positive woolly fibers in the forebrain of the rhesus monkey. *Neuroscience*, 39(2), 323–338.
- Heimer, L., Alheid, G. F., de Olmos, J. S., Groenewegen, H. J., Haber, S. N., Harlan, R. E., & Zahm, D. S. (1997). The accumbens: Beyond the core-shell dichotomy. *The Journal of Neuropsychiatry and Clinical Neurosciences*, 9(3), 354–381.
- Heimer, L., Zahm, D. S., Churchill, L., Kalivas, P. W., & Wohltmann, C. (1991). Specificity in the projection patterns of the accumbal core and shell in the rat. *Neuroscience*, 41(1), 89–125.
- Ikeda, H., Saigusa, T., Kamei, J., Koshikawa, N., & Cools, A. R. (2013). Spiraling dopaminergic circuitry from the ventral striatum to dorsal striatum is an effective feed-forward loop. *Neuroscience*, 241, 126–134.
- Ikemoto, S. (2007). Dopamine reward circuitry: Two projection systems from the ventral midbrain to the nucleus accumbens-olfactory tubercle complex. *Brain Research Reviews*, 56(1), 27–78.
- Kajiwara, R., Wouterlood, F. G., Sah, A., Boekel, A. J., Baks-Te Bulte, L. T. G., & Witter, M. P. (2008). Convergence of entorhinal and CA3 inputs onto pyramidal neurons and interneurons in hippocampal area CA1. An anatomical study in the rat. *Hippocampus*, 18(3), 266–280.
- Kelley, A. E., Baldo, B. A., & Pratt, W. E. (2005). A proposed hypothalamic-thalamic-striatal axis for the integration of energy balance, arousal, and food reward. *The Journal of Comparative Neurology*, 493(1), 72–85.
- Keramati, M., & Gutkin, B. (2013). Imbalanced decision hierarchy in addicts emerging from drug-hijacked dopamine spiraling circuit. *PLoS One*, 8(4), e61489.
- Mailly, P., Aliane, V., Groenewegen, H. J., Haber, S. N., & Deniau, J. M. (2013). The rat prefrontal system analyzed in 3D: Evidence for multiple interacting functional units. *The Journal of Neuroscience*, 33(13), 5718–5727.
- Mailly, P., Charpier, S., Mahon, S., Menetrey, A., Thierry, A. M., Glowinski, J., & Deniau, J. M. (2001). Dendritic arborizations of the rat substantia nigra pars reticulata neurons: Spatial organization and relation to the lamellar compartmentation of striato-nigral projections. *The Journal of Neuroscience*, 21(17), 6874–6888.
- Maurice, N., Deniau, J. M., Menetrey, A., Glowinski, J., & Thierry, A. M. (1997). Position of the ventral pallidum in the rat prefrontal cortex-basal ganglia circuit. *Neuroscience*, 80(2), 523–534.
- Maurice, N., Deniau, J. M., Menetrey, A., Glowinski, J., & Thierry, A. M. (1998). Prefrontal cortex-basal ganglia circuits in the rat: Involvement of ventral pallidum and subthalamic nucleus. *Synapse*, 29(4), 363–370.
- Maurin, Y., Banrezes, B., Menetrey, A., Mailly, P., & Deniau, J. M. (1999). Three dimensional distribution of nigrostriatal neurons in the rat: Relation to the topography of striatonigral projections. *Neuroscience*, 91(3), 891–909.
- Menegas, W., Bergan, J. F., Ogawa, S. K., Isogai, Y., Umadevi Venkataraju, K., Osten, P., ... Watabe-Uchida, M. (2015). Dopamine neurons projecting to the posterior striatum form an anatomically distinct subclass. *eLife*, 4, e10032.
- Mogenson, G. J., Jones, D. L., & Yim, C. Y. (1980). From motivation to action: Functional interface between the limbic system and the motor system. *Progress in Neurobiology*, 14, 69–97.
- Montaron, M. F., Deniau, J. M., Menetrey, A., Glowinski, J., & Thierry, A. M. (1996). Prefrontal cortex inputs of the nucleus accumbens-nigrothalamic circuit. *Neuroscience*, 71(2), 371–382.
- Morales, M., & Margolis, E. B. (2017). Ventral tegmental area: Cellular heterogeneity, connectivity and behaviour. *Nature Reviews. Neuroscience*, 18(2), 73–85.
- Nauta, W. J., Smith, G. P., Faull, R. L., & Domesick, V. B. (1978). Efferent connections and nigral afferents of the nucleus accumbens septi in the rat. *Neuroscience*, 3(4–5), 385–401.
- Parent, A., Charara, A., & Pinault, D. (1995). Single striatofugal axons arborizing in both pallidal segments and in the substantia nigra in primates. *Brain Research*, 698(1–2), 280–284.
- Paxinos, G., & Watson, C. (2005). *The rat brain in stereotaxic coordinates* (5th ed.). New York: Elsevier-Academic Press.
- Rasband, W. S. (1997–2006). *ImageJ*. Bethesda, MD: U.S. National Institute of Health. Retrieved from <http://rsb.info.nih.gov/ij/>
- Richard, J. M., Castro, D. C., Difeliceantonio, A. G., Robinson, M. J., & Berridge, K. C. (2013). Mapping brain circuits of reward and motivation: In the footsteps of Ann Kelley. *Neuroscience & Biobehavioral Reviews*, 37(9), 1919–1931.
- Rosene, D. L., Roy, N. J., & Davis, B. J. (1986). A cryoprotection method that facilitates cutting frozen sections of whole monkey brains for histological and histochemical processing without freezing artifact. *Journal of Histochemistry & Cytochemistry*, 34(10), 1301–1315.
- Saddoris, M. P., Wang, X., Sugam, J. A., & Carelli, R. M. (2016). Cocaine self-administration experience induces pathological phasic accumbens dopamine signals and abnormal incentive behaviors in drug-abstinent rats. *The Journal of Neuroscience*, 36(1), 235–250.
- Sesack, S. R., & Grace, A. A. (2010). Cortico-basal ganglia reward network: Microcircuitry. *Neuropsychopharmacology*, 35(1), 27–47.
- Sesack, S. R., & Pickel, V. M. (1992). Prefrontal cortical efferents in the rat synapse on unlabeled neuronal targets of catecholamine terminals in the nucleus accumbens septi and on dopamine neurons in the

- ventral tegmental area. *The Journal of Comparative Neurology*, 320(2), 145–160.
- Shi, C., & Cassell, M. D. (1993). Combination of intracellular staining of retrogradely labeled neurons and anterograde fluorescent tracing: Use of the confocal laser scanning microscope. *The Journal of Neuroscience Methods*, 47(1–2), 23–31.
- Somogyi, P., Bolam, J. P., Totterdell, S., & Smith, A. D. (1981). Monosynaptic input from the nucleus accumbens–ventral striatum region to retrogradely labelled nigrostriatal neurones. *Brain Research*, 217(2), 245–263.
- Tepper, J. M., & Lee, C. R. (2007). GABAergic control of substantia nigra dopaminergic neurons. *Progress in Brain Research*, 160, 189–208.
- Thierry, A. M., Van Dongen, Y. C., Kolomiets, B., Glowinski, J., Groenewegen, H. J., & Deniau, J. M. (2002). Mesencephalic dopamine neurons as an interface between the ventral and dorsal striatum: Anatomical and electrophysiological evidence. *FENS*, Abstract 1:A369.
- Tripathi, A., Prensa, L., Cebrián, C., & Mengual, E. (2010). Axonal branching patterns of nucleus accumbens neurons in the rat. *The Journal of Comparative Neurology*, 518(22), 4649–4673.
- Tripathi, A., Prensa, L., & Mengual, E. (2013). Axonal branching patterns of ventral pallidal neurons in the rat. *Brain Structure & Function*, 218(5), 1133–1157.
- Usuda, I., Tanaka, K., & Chiba, T. (1998). Efferent projections of the nucleus accumbens in the rat with special reference to subdivision of the nucleus: Biotinylated dextran amine study. *Brain Research*, 797(1), 73–83.
- van Dongen, Y. C., Kolomiets, B. P., Groenewegen, H. J., Thierry, A. M., & Deniau, J. M. (2009). A subpopulation of mesencephalic dopamine neurons interfaces the shell of nucleus accumbens and the dorsolateral striatum in rats. In H. J. Groenewegen, P. Voorn, H. W. Berendse, A. B. Mulder, & A. R. Cools (Eds.), *The basal ganglia IX. Advances in behavioral biology* (Vol. 58, pp. 119–130). Berlin: Springer.
- Volman, S. F., Lammel, S., Margolis, E. B., Kim, Y., Richard, J. M., Roitman, M. F., & Lobo, M. K. (2013). New insights into the specificity and plasticity of reward and aversion encoding in the mesolimbic system. *The Journal of Neuroscience*, 33(45), 17569–17576.
- Voorn, P., Vanderschuren, L. J., Groenewegen, H. J., Robbins, T. W., & Pennartz, C. M. (2004). Putting a spin on the dorsal-ventral divide of the striatum. *Trends in Neurosciences*, 27(8), 468–474.
- Wassef, M., Berod, A., & Sotelo, C. (1981). Dopaminergic dendrites in the pars reticulata of the rat substantia nigra and their striatal input. Combined immunocytochemical localization of tyrosine hydroxylase and anterograde degeneration. *Neuroscience*, 6(11), 2125–2139.
- Willuhn, I., Burgeno, L. M., Everitt, B. J., & Phillips, P. E. M. (2012). Hierarchical recruitment of phasic dopamine signaling in the striatum during the progression of cocaine use. *Proceedings of National Academy of Sciences of the United States of America*, 109(50), 20703–20708.
- Willuhn, I., Burgeno, L. M., Groblewski, P. A., & Phillips, P. E. (2014). Excessive cocaine use results from decreased phasic dopamine signaling in the striatum. *Nature Neuroscience*, 17(5), 704–709.
- Wouterlood, F. G. (2006). Combined fluorescence methods to determine synapses in the light microscope: Multilabel confocal laserscanning microscopy. In L. Zaborszky, F. G. Wouterlood, & J. L. Lanciego (Eds.), *Neuroanatomical tract-tracing 3: Molecules - neurons - systems* (pp. 394–435). New York: Springer.
- Wouterlood, F. G., & Beliën, J. A. M. (2014). Translation, touch and overlap in multi-fluorescence confocal laser scanning microscopy to quantify synaptic connectivity. In L. Bakota & R. Brandt (Eds.), *Laser scanning microscopy and quantitative image analysis of neuronal tissue. Neuromethods* (Vol. 87, pp. 1–36). New York, NY: Humana Press.
- Wouterlood, F. G., Bloem, B., Mansvelter, H. D., Luchicchi, A., & Deisseroth, K. (2014). The fourth generation of neuroanatomical tracing techniques: Exploiting the offspring of genetic engineering. *Journal of Neuroscience Methods*, 235, 331–348.
- Wouterlood, F. G., Goede, P. H., Arts, M. P., & Groenewegen, H. J. (1992). Simultaneous characterization of efferent and afferent connectivity, neuroactive substances, and morphology of neurons. *The Journal of Histochemistry and Cytochemistry*, 40(4), 457–465.
- Wouterlood, F. G., & Groenewegen, H. J. (1985). Neuroanatomical tracing by use of *Phaseolus vulgaris*-leucoagglutinin (PHA-L): Electron microscopy of PHA-L-filled neuronal somata, dendrites, axons and axon terminals. *Brain Research*, 326(1), 188–191.
- Wouterlood, F. G., van Denderen, J. C. M., Blijleven, N., van Minnen, J., & Härtig, W. (1998). Two-laser dual-immunofluorescence confocal laser scanning microscopy using Cy2- and Cy5-conjugated secondary antibodies: Unequivocal detection of co-localization of neuronal markers. *Brain Research Protocols*, 2(2), 149–159.
- Wright, C. I., Beijer, A. V., & Groenewegen, H. J. (1996). Basal amygdaloid complex afferents to the rat nucleus accumbens are compartmentally organized. *The Journal of Neuroscience*, 16(5), 1877–1893.
- Xia, Y., Driscoll, J. R., Wilbrecht, L., Margolis, E. B., Fields, H. L., & Hjelmstad, G. O. (2011). Nucleus accumbens medium spiny neurons target non-dopaminergic neurons in the ventral tegmental area. *The Journal of Neuroscience*, 31(21), 7811–7816.
- Yetnikoff, L., Lavezzi, H. N., Reichard, R. A., & Zahm, D. S. (2014). An update on the connections of the ventral mesencephalic dopaminergic complex. *Neuroscience*, 282, 23–48.
- Yin, H. H., Mulcare, S. P., Hilário, M. R. F., Clouse, E., Holloway, T., Davis, M. I., ... Costa, R. M. (2009). Dynamic reorganization of striatal circuits during the acquisition and consolidation of a skill. *Nature Neuroscience*, 12(3), 333–341.
- Zahm, D. S., Cheng, A. Y., Lee, T. J., Ghobadi, C. W., Schwartz, Z. M., Geisler, S., ... Veh, R. W. (2011). Inputs to the midbrain dopaminergic complex in the rat, with emphasis on extended amygdala-recipient sectors. *The Journal of Comparative Neurology*, 519(16), 3159–3188.

How to cite this article: Wouterlood FG, Engel A, Daal M, et al. Mesencephalic dopamine neurons interfacing the shell of nucleus accumbens and the dorsolateral striatum in the rat. *J Neuro Res*. 2018;96:1518–1542. <https://doi.org/10.1002/jnr.24242>